UNIVERSITAT POLITÈCNICA DE VALÈNCIA

UNIVERSITAT POLITÈCNICA DE VALÈNCIA

Plant Molecular and Cellular Biology Joint Research Institute (IBMCP)

Local auxin biosynthesis shapes root architecture in response to environmental cues.

Master's Thesis

Master's Degree in Plant Molecular and Cellular Biotechnology

AUTHOR: Noya Falcón, Xulia

Tutor: Agusti Feliu, Javier

Experimental director: Brumós Fuentes, Javier

ACADEMIC YEAR: 2024/2025

Abstract

Plants exhibit a remarkable capacity to integrate external environmental cues with their own internal developmental programs to always adapt their growth and development to dynamic conditions. This adaptive ability has been shaped over millions of years of evolution and increasingly underscores the key role plant hormones play in the information integration process.

Auxin is a fundamental plant hormone accountable for many aspects of plant development and its regulation in response to environmental variations. In other words, auxin contributes to the adaption of plants to different environments or conditions. Auxin morphogenic gradients govern stem cell niches and cellular differentiation, determining cell fate. The polar transport of auxin is essential for creating and maintaining the auxin gradients. However, recent discoveries highlighting the refined spatiotemporal expression patterns of auxin biosynthesis genes, such as the *TAA1/TAR* and *YUC* families, suggest that local auxin biosynthesis also has a major contribution to the formation of the auxin gradients.

In this study, we investigate the effects of temperature in root development and its relationship with auxin production in *Arabidopsis thaliana*. Trought phenotypic analyses, *DR5* reporter expression, and gene expression levels analysis of IAA biosynthesis and catabolism genes, we examined the role of local auxin biosynthesis under increasing temperature conditions.

Elevated temperatures affected root architecture through changes in primary root growth and number of lateral roots formed. Thermomorphegenesis temperature promotes growth and the formation of lateral roots. Whereas, higher temperatures caused inhibition of growth and a significantly reduction of lateral root number.

DR5 expression indicates differential auxin responses to increasing temperatures. Interestingly, the expression levels of *DR5* under different temperatures only partially correlate with the biosynthesis genes levels of expression.

The observed discrepancies between auxin response and biosynthesis levels suggest that additional regulatory mechanisms may play a role in modulating auxin responses and/or auxin levels under these temperature conditions in the root system.

Therefore, we have investigated the expression levels of auxin catabolism genes and performed *in silico* analyses to identify candidate transcription factors that may regulate auxin levels.

Key words: plant development; local auxin biosynthesis; root architecture; thermomorphogenesis; heat stress; *Arabidopsis thaliana*; transcriptional regulation.

Sustainable Development Goals

Objetivos de Desarrollo Sostenibles	Alto	Medio	Bajo	No procede
ODS 1. **Fin de la pobreza.**			✓	
ODS 2. **Hambre cero.**	✓			
ODS 3. **Salud y bienestar.**		✓		
ODS 4. **Educación de calidad.**				✓
ODS 5. **Igualdad de género.**				✓
ODS 6. **Agua limpia y saneamiento.**			✓	
ODS 7. **Energía asequible y no contaminante.**				✓
ODS 8. **Trabajo decente y crecimiento económico.**				✓
ODS 9. **Industria, innovación e infraestructuras.**				✓
ODS 10. **Reducción de las desigualdades.**				✓
ODS 11. **Ciudades y comunidades sostenibles.**				✓
ODS 12. **Producción y consumo responsables.**				✓
ODS 13. **Acción por el clima.**	✓			
ODS 14. **Vida submarina.**			✓	
ODS 15. **Vida de ecosistemas terrestres.**	✓			
ODS 16. **Paz, justicia e instituciones sólidas.**				✓
ODS 17. **Alianzas para lograr objetivos.**				✓

Descripción de la alineación del TFG/TFM con los ODS con un grado de relación más alto.

The present research aims to elucidate the molecular mechanisms underlying the *Arabidopsis* root´s response to elevated temperatures. The knowledge gained from this study will contribute to the development of crop varieties that are more resistant to extreme climatic conditions. The results obtained support global efforts to achieve the Sustainable Development Goals:

- ✓ ODS2. Food security
- ✓ ODS3. Health and well-being
- ✓ ODS13. Climate action
- ✓ ODS15. Conservation of terrestrial ecosystems

Acknowledgements

La realización de este Trabajo Fin de Máster supuso un reto para mí desde el primer minuto que pisé el laboratorio. Es por ello, que me gustaría agradecer a todas las personas que formaron parte de este proceso, directa o indirectamente, porque no habría sido posible sin ellas.

En primer lugar, quiero agradecer a mi tutor Javier Brumós por todo lo que me ha enseñado. Sin duda su dedicación y compromiso para orientarme en todo momento durante el desarrollo de este trabajo ha sido imprescindible para llevarlo a cabo.

Asimismo, agradezco a todos los integrantes del Brumos lab y Agustí lab por su ayuda y generosidad cuando estaba perdida, así como por todos los ratitos de conversación que hacían las horas de trabajo más livianas. En especial, me gustaría agradecer a mis *fifes* Enrique y Damiano, por siempre sacar un hueco en ayudarme cuando lo necesitaba, por compartir los momentos de descanso y por esa paella y pasta italiana que siempre se posponen.

Por otro lado, no podría no agradecer a mis compañeros del máster. Hace poco más de un año que nos conocemos, pero sin duda han sido un gran pilar en esta etapa. Desde los momentos compartidos en nuestras tardes de clase, nuestras paradas por los pasillos cada vez que nos encontrábamos (aunque fuéramos cargados de cosas por hacer), de las comidas que alargábamos hasta el último minuto, los abrazos de ánimos cuando flaqueaban las fuerzas y los muchos momentos de playa, terrazas, cine y fiesta de los que tanto disfrutamos. Y, aunque me gustaría poder mencionar a todos ellos, me gustaría agradecer especialmente a Ave, por su bondad y generosidad, por todas las historias compartidas (y las que nos quedan) y por ser casa también, a Lorenzo, por estar siempre, por los paseos en el Golfito escuchando desde *Las Chuches* hasta *La Raíz*, por los caminos de vuelta a casa y los té matcha, a Carla, por todas las visitas al laboratorio, su risa contagiosa, y por nuestras mil y una charlas, y a Andrea, por todos los cafés compartidos, por creer en mí cuando yo no lo veía y, en definitiva, por ser mi cómplice y confidente todo este año.

Para ir finalizando, no podría terminar sin darle infinitas gracias a mis amigos y familia que, aún a más de mil kilómetros de distancia, siempre me transmitieron su fuerza. Porque no dudan de mí, porque me apoyan en todos los pasos que voy dando, y porque siempre me reciben con el mayor de los abrazos cuando vuelvo a casa. Especialmente, agradezco a mi abuela por toda la sabiduría, calma y amor que transmite en cada segundo que pasas a su lado.

Y por último y más importante, quiero agradecerle *á miña nai* – mi madre – por todo lo que hace por mí cada día, por haber puesto todas sus fuerzas (y más) en darme una vida llena de oportunidades, de amor, de libertad. Siempre ha sido una referencia que seguir, un lugar al que volver, un impulso para enfrentarme a nuevas experiencias. Y porque sé que a pesar de no entender ni una palabra de este manuscrito, lo leerá de arriba abajo y, con su mirada de orgullo, me dirá que está perfecto. *Quérote moito.*

Table of content

Table of figures

Abbreviations

IBA Indole-3-butyric acid

1-NAA 1-naphthylacetic acid

2,4-D 2,4-dichlorophenoxyacetic acid

4-Cl-IAA 4-Chloroindole-3-acetic acid

ABA Abscisic acid

ACC 1-aminocyclopropane-1-carboxylic acid

AUX1 AUXINE-1

CHIP-seq Chromatin Immunoprecipitation followed by Sequencing

CK Cytokines

DAO1 DIOXYGENASE FOR AUXIN OXIDATION 1

DAP-seq DNA Affinity Purification Sequencing

DMSO Dimethyl sulfoxide

GH3 GRETCHEN HAGEN 3

GUS β-Glucuronidase

IAA Indole-3-acetic acid

IAM Indole-3-acetamide

IAOx Indole-3-acetaldoxime

IPyA Indole-3-pyruvic acid

IQR Interquartile range

JA Jasmonic acid

NPA N-1-naphthylphthalamic acid

PIN PIN-FORMED

QC Quiescent center

scRNA-seq Single Cell RNA-Sequencing

TAA1/TARs TRYPTOPHAN AMINOTRANSFERASE

TF Transcription factor

Trp Tryptophan

WEI8 WEAK INSENSITIVE ETHYLENE 8

WT Wild type

YUCs YUCCA flavin monooxygenase

1. Introduction

1.1. Auxin: key phytohormone in root architecture plasticity

The term *auxins* (from the Greek 'αυξειν,' meaning 'to grow') refers to a group of structurally related chemical compounds that act as essential hormones in plants. Some of the natural auxins that have been identified include indole-3-butyric acid (IBA) and 4-chloroindole-3-acetic acid (4-Cl-IAA), although the most common and abundant auxin is indole-3-acetic acid (IAA). In addition, there are synthetic auxins, such as 1-naphthylacetic acid (1-NAA) and 2,4-dichlorophenoxyacetic acid (2,4-D), which are extensively applied in agriculture (Tanaka et al., 2006).

Auxins accumulate in specific cell types, establishing concentration gradients that coordinate a range of developmental processes in plants, such as embryogenesis, the establishment of apical-basal polarity, hypocotyl elongation, flowering, and tropic responses (Mashiguchi et al., 2011; Zhang et al., 2022). Among the physiological roles of auxins, their significance in the development and maintenance of the root system is particularly notable, including the formation and growth of lateral roots, as well as the regulation of root angle (Karlova et al., 2021; Overvoorde et al., 2010). Specifically, in the root meristem, auxins regulate cell division rates, elongation, and differentiation, ultimately shaping root architecture and function (Brumos et al., 2018)

The root system is essential for the overall functioning of plants, serving as the main source for water and mineral uptake from the soil, as well as a pathway for communication with the soil microbiome and neighbouring plants (Karlova et al., 2021). Their remarkable plasticity allows roots to adapt to environmental changes by undergoing physiological and morphological modifications, many of which are regulated by auxin (Calleja-Cabrera et al., 2020).

In *Arabidopsis thaliana* (*A. thaliana*), the primary root comprises four distinct longitudinal zones (Figure 1): meristematic or division zone, transition zone, elongation zone, and differentiation zone (Muraro et al., 2013). The various cell types in the root originate from a group of slowly dividing cells located in the root meristem, known as the quiescent center (QC) (Brady et al., 2007; González-García et al., 2023). The QC maintains a niche of stem cells, controlling the differentiation rates into various cell types and ensuring proper development of root system. This regulation is controlled by auxin levels (Stepanova et al., 2008).

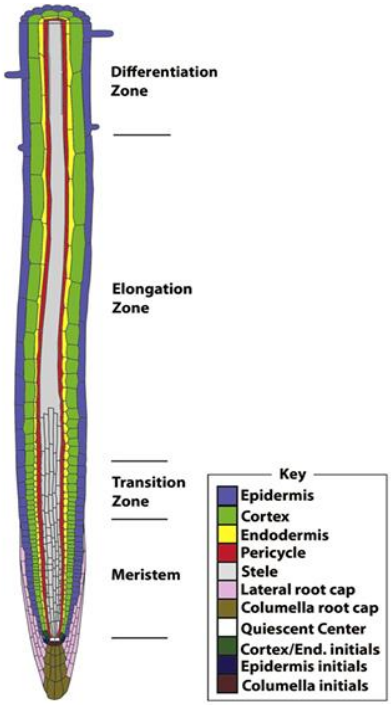

Figure 1. A schematic representation of the root of *A. thaliana*

Muraro et al. (2013)

1.2. Thermomorphogenesis and heat stress in *Arabidopsis* roots

Climate change is impacting agricultural systems, mainly due to the increase of global temperatures and the effect on precipitation patterns. These changes, combined with intensive agricultural practices, have degraded soils and intensify abiotic stresses, which are responsible for significant reductions in crop yields (González-García et al., 2023; Karlova et al., 2021). While most research has been focused to understanding plant shoot responses to elevated temperatures, root responses remain comparatively understudied. Roots are critical for water and nutrient uptake, anchoring the plant, and interacting with the soil. Thus, understanding root responses to high temperatures is essential for developing resilient crops and optimizing root system architecture to sustain productivity in a warming world (Calleja-Cabrera et al., 2020).

Thermomorphogenesis refers to morphological changes induced by mild increases in ambient temperature, within the range of 12 ºC to 28 °C in *Arabidopsis* (Fonseca de Lima et al., 2021). In shoots, thermomorphogenesis includes elongation of the hypocotyl, petioles, and leaves, which are well-documented. In contrast, root thermomorphogenesis is less understood, despite evidence that roots exhibit thermomorphogenesis responses such as primary root elongation or an open architecture. These responses are interpreted as a way for roots to grow deeper and reach cooler soil layers (Bellstaedt et al., 2019; Karlova et al., 2021; Ai et al., 2023). Auxin plays a central role in regulating thermomorphogenesis and high temperatures can influence auxin biosynthesis, transport and signaling, which increase division cell rates and elongation. Furthermore, there is evidence that roots can autonomously sense and respond to temperature changes independently of the shoot, suggesting unique regulatory pathways that require further exploration (Ai et al., 2023).

When temperatures exceed the thermomorphogenic range, plants experience heat stress, which disrupts root growth and development. Heat stress affects to protein folding, enzyme activity, membrane integrity, and cellular organization. These can impair root development, leading to reduced primary root length, fewer lateral roots, and reduced nutrient and water uptake (Fonseca de Lima et al., 2021; Tiwari et al., 2021). Phytohormones, particularly auxin, play a crucial role in maintaining root growth under heat stress. However, high temperatures often disrupt auxin levels and distribution, further affecting root responses (Agusti et al., 2021; Ai et al., 2023). Roots also exhibit physiological plasticity, such as increased root hair density and elongation, to enhance soil exploration and resource acquisition under adverse conditions (Calleja-Cabrera et al., 2020).

Roots are integral to plant resilience under high-temperature conditions and exhibit a remarkable capacity for autonomous sensing and response to elevated temperatures. Their capacity to independently sense and adapt to high temperatures underscores the need for more focused research on root thermomorphogenesis and heat stress responses. Understanding these processes will be vital for breeding stress-resilient crops with optimized root systems capable of thriving in increasingly extreme conditions.

1.3. Auxin biosynthesis and its regulation: genetic pathways

Since their discovery in the early 20th century, auxins have been a focal point of plant hormone research. Although substantial efforts have been dedicated to understanding plant responses to auxin and its transport in the last decades, the molecular mechanisms underlying auxin production remain poorly characterized (Brumos et al., 2014).

Currently, two main types of IAA biosynthesis pathways are known: the tryptophan-independent (Trp-independent) pathway and the tryptophan-dependent (Trp-dependent) pathway. The Trp-independent pathways remain poorly understood, while the Trp-dependent pathways are better characterized. Among the Trp-dependent pathways, three routes have been identified: the indole-3-acetaldoxime (IAOx), indole-3-acetamide (IAM), and indole-3-pyruvic acid (IPyA) pathways (Brumos et al., 2014).

In this study, we focus on the genes involved in the IPyA pathway the main route for IAA synthesis in plants (Figure 2). The IPyA pathway is the only fully characterized route and consists of two steps involving the *TRYPTOPHAN AMINOTRANSFERASE* (*TAA1/TARs*) and the *YUCCA* family of flavin monooxygenases (*YUCs*) gene families (Won et al., 2011). Specifically, in *A. thaliana*, the *TAA1*, *TAR1*, and *TAR2* are central to the first step, while 11 members of the *YUC* family (*YUC1 – 11*) are implicated in the second step (Mashiguchi et al., 2011).

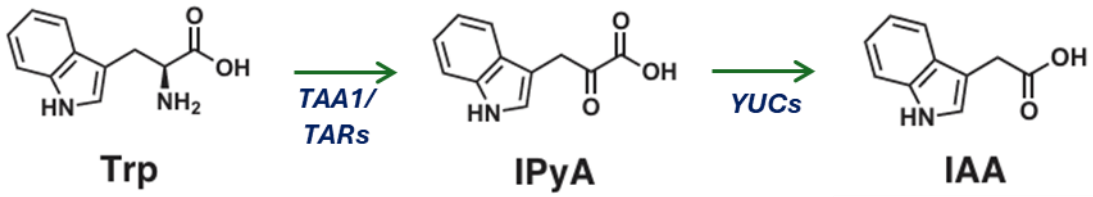

Figure 2. IPyA pathway in *A. thaliana*

Adapted from Sato et al. (2022)

The first step of the IPyA pathway involves the conversion of Trp into the intermediate IPyA, a reaction catalyzed by the aminotransferases TAA1/TARs. These enzymes are evolutionarily conserved across plant species, being present in a wide range of mosses (e.g., *Physcomitrella*), monocots (e.g., *Zea mays*), and dicots (e.g., *A. thaliana*) (Stepanova et al., 2011).

In the second step, YUCs mediate the conversion of IPyA into active IAA. This step is a key regulatory point in IAA biosynthesis because the activity of the 11 *YUCs* genes are the rate-limiting step of the whole IPyA pathway (Mashiguchi et al., 2011).

The role of the auxin biosynthesis genes *TAA1/TARs* and *YUCs* is crucial, as they are involved in fundamental physiological processes, including embryogenesis, seedling growth, floral development, and lateral root formation (Mashiguchi et al., 2011). Evidence supporting their importance has been obtained from studies on loss-of-function mutants. For example, *TAA1/TARs* mutants, such as *wei8-1 tar2-1* (Figure 3), exhibit abrupt phenotypic changes in flower development, leading to sterility (Won et al., 2011). *WEI8* (*WEAK ETHLYNE INSENSITIVE 8*) corresponds to *TAA1*, which was renamed in Stepanova *et al.* (2008) for the characterization of the protein defective in *wei8*.

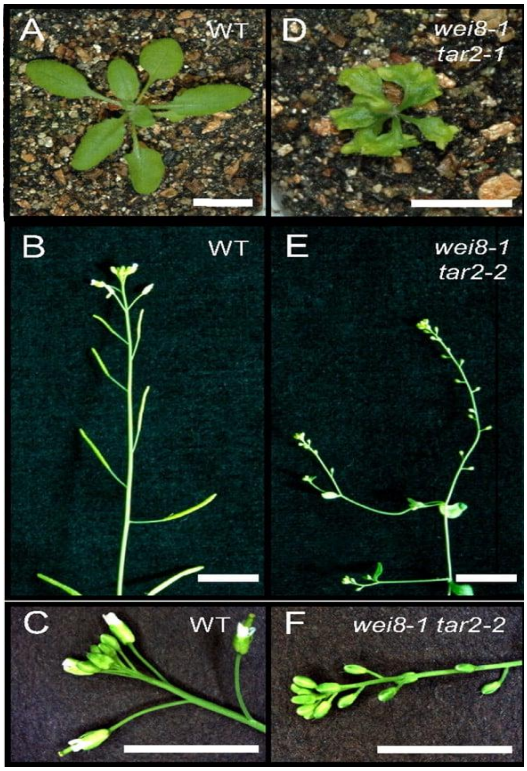

Figure 3. Phenotypes of TAA1/TARs-deficient mutants. (A) WT seedlings. **(B)** Upper region and **(C)** inflorescence of WT plants. **(D)** Seedlings of *wei8-1 tar2-1* mutants. **(E)** Upper region and **(F)** inflorescence of *wei8-1 tar2-2* mutants**.**

Adapted from Mashiguchi et al. 2011

Similarly, multiple *YUCs* loss-of-function mutants display severe developmental defects (Figure 4). A notable example is the quintuple mutant *yuc3yuc5yuc7yuc8yuc9*, which shows disrupted gravitropism and impaired primary root growth (Cao et al., 2019). In addition, *YUC1* overexpression mutants exhibit a characteristic phenotype, including elongated hypocotyls and enhanced apical dominance, which are indicative of elevated IAA concentrations. These observations further highlight the critical role of biosynthesis genes and auxin in plant development (Mashiguchi et al., 2011).

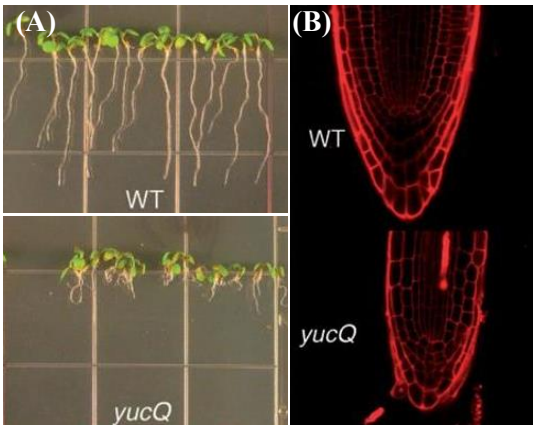

Figure 4. *Knockout* mutants of *YUCs* show a characteristic phenotype. (A) Quintuple mutant (*yucQ*) displays dramatic defects in *Arabidopsis* root development. **(B)** The *yucQ* roots have a smaller root cap and an abormal meristem

Adapted from Chen et al. (2014)

The IPyA pathway requires precise regulation to maintain cellular homeostasis and optimal auxin levels. Despite the physiological significance of IAA biosynthesis regulation, the mechanisms governing the coordination and regulation of *TAA1/TARs* and *YUCs* remain poorly understood (Sato et al., 2022).

The primary regulatory mechanisms of this pathway occur at transcriptional level, post-transcriptional level, protein modification, and negative feedback loop (Luo & Di, 2023). Regarding negative feedback regulation, it has been proposed that IPyA itself acts as an inhibitor of TAA1 enzymatic activity (Sato et al., 2022). On the other hand, transcriptional regulation is notably influenced by epigenetic modifications, such as DNA methylation, playing a key role in modulating auxin levels. Furthermore, transcription factors (TFs) also contribute activating or repressing gene expression, ensuring appropriate IAA

homeostasis. Notable examples include MYC, which activates *YUC8/9* in response to mechanical wounding, and ARR1 and EIN3, which enhance *TAA1* expression (Luo & Di, 2023).

These regulatory processes are also modulated by environmental conditions and hormonal signalling. In terms of hormonal regulation, ethylene-mediated root growth plays a vital role in maintaining specific auxin production patterns. Additionally, other hormones such as jasmonate (JA), abscisic acid (ABA), and cytokinins (CK) significantly influence the regulation of *TAA1/TARs* and *YUCs* biosynthetic genes. Finally, environmental factors, such as increased temperature, can alter the regulation of IAA synthesis, altering the expression patterns of *TAA1* and *YUC8* (Brumos et al., 2014).

1.4. The spatiotemporal expression patterns of auxin biosynthesis genes

The spatiotemporal accumulation of auxin, and consequently of its biosynthetic genes, is asymmetric and plays a crucial role in facilitating the developmental changes necessary for plant growth. This expression varies depending on environmental conditions and the physiological functions required. For instance, during embryogenesis, the distribution of auxins differs from that observed during post-embryonic organ formation, such as the development of lateral roots (Tanaka et al., 2006).

Various methodologies are used to study the spatiotemporal expression of auxins, with the *DR5* reporter gene being one of the most prominent tools. *DR5* is a synthetic promoter composed of multiple TGTCTC repeats, an auxin-responsive element (Ulmasov et al., 1997; Wong et al., 2023). Consequently, it serves as an indirect indicator of auxin levels in cells. To visualize and quantify its activity, *DR5* has been fused to the *β-glucuronidase* gene that encodes for the GUS enzyme which produces a blue coloration in regions where DR5 drives its expression (Tanaka et al., 2006; Wong et al., 2023).

These auxin patterns are established through a combination of local biosynthesis and transport mechanisms, which together generate a gradient essential for regulating distinct biological responses across various organs and environmental conditions ((Blakeslee et al., 2019; Wong et al., 2023).

Polar auxin transport is the directed movement of auxins from the apical aerial region toward the basal parts of the plant through the vasculature. This process is predominantly unidirectional and plays a key role in distributing auxins throughout the plant. Additionally, auxin transport also occurs through a cell-apoplast-cell pathway, governed by the chemiosmotic model.

This model describes the transport of auxins facilitated by carrier proteins, addressing the challenge posed by the protonation state of IAA. IAA exists in two forms: protonated (IAA-H) or deprotonated (IAA^-). The protonated form can passively diffuse across the plasma membrane, while the deprotonated form requires active transport. Influx carrier proteins, such as AUXINE1 (AUX1), enable the uptake of IAA-H into cells, whereas efflux carrier proteins, including the PIN-FORMED (PIN) family, direct the export of IAA^- to establish and

maintain auxin gradients. These coordinated transport mechanisms are critical for maintaining auxin gradients, which regulate diverse developmental processes such as cell elongation, vasculature development or organogenesis (Tanaka et al., 2006).

An example of how auxin biosynthesis gene expression patterns are modulated is observed in the phenomenon of hydropatterning. Hydropatterning describes the asymmetric emergence of lateral roots when only one side of the root is in contact with water, while the opposite side is in contact with air. This process is driven by an increase in the expression of the *TAA1* auxin biosynthesis gene in the epidermal cells in contact to water. Simultaneously, there is an upregulation of specific auxin transporters, particularly PIN2, PIN3, and PIN7, which generate an auxin gradient favoring lateral root formation on the water-exposed side (Wong et al., 2023).

1.5. Local auxin biosynthesis

Canonically, polar auxin transport from the aerial parts to the root system has been studied as the primary mechanism responsible for establishing the auxin gradient necessary for developmental processes, with PIN proteins playing a critical role (Geisler, 2021). However, it has been demonstrated that polar auxin transport alone is insufficient to maintain the maximum auxin gradient in tissues (Zhao, 2018).

Local auxin biosynthesis and polar auxin transport are both required to achieve an optimal auxin gradient, functioning as a redundant mechanism to ensure adequate auxin levels (Brumos et al., 2018). This redundancy is essential for maintaining root meristematic activity in *Arabidopsis*, where the QC plays a fundamental role in regulating cell differentiation rates in the cell types, necessary to establish proper root architecture. Auxins plays an essential role in this process, as demonstrated by the high expression of *TAA1* in the QC, which underscore the significance role of local auxin biosynthesis for maintaining root meristem activity (Stepanova et al., 2008).

The critical role of local auxin biosynthesis in the development of the primary root has been extensively analyzed by Brumos et al. (2018) through different approaches. Using grafting, it was shown that a wild-type (WT) shoot cannot rescue the *wei8-1 tar2-1* double mutant root defects. The grafted plants exhibit a compromised phenotype in all the root system, which indicates that auxin transported from the shoot to the root is insufficient to maintain a functional root meristem.

On the other hand, when auxin biosynthesis inhibitors such as kynurenine (inhibitor of *TAA1/TARs*) and yucasin (inhibitor of *YUCs*) were applied in WT roots, the addition of exogenous IAA to the shoot failed to restore functionality in root meristem. Thus, roots exhibit non-functional meristems, and lateral roots also being affected by the inability to locally produce IAA in the root.

While polar auxin transport is necessary to establish the auxin gradient, it has been demonstrated that local auxin biosynthesis in the QC alone is sufficient to maintain root meristem functionality (Figure 5). This was confirmed through experiments using the auxin transport inhibitor N-1-naphthylphthalamic acid (NPA). Specifically, QC-

specific promoters, such as *WOX5*, was used to show that local auxin biosynthesis within the QC can sustain a functional root meristem, even when auxin transport is blocked (Brumos et al., 2018).

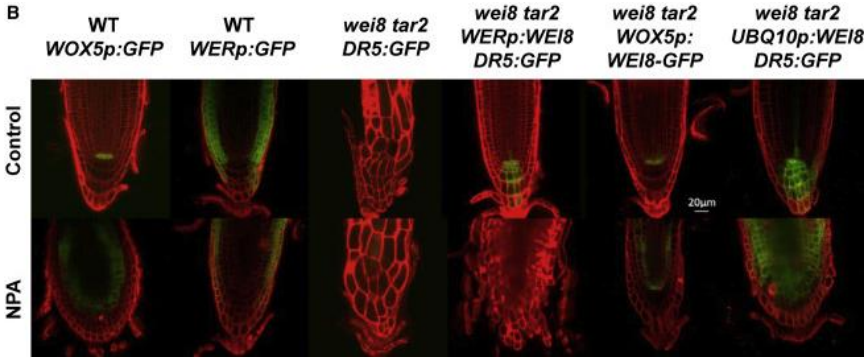

Figure 5. Local auxin biosynthesis in the QC is required and sufficient for root meristem maintenance. Confocal microscopy of *Arabidopsis* root tips showing the expression of marker genes of WT and *wei8 tar2* mutants. Scale bar= 20µm

Brumos et al (2018)

There is also evidence that local expression of *YUC* genes in the roots of *Arabidopsis*, such as *YUC3*, *YUC7*, and *YUC8*, is crucial for maintaining the root meristem and ensuring its proper development. This was demonstrated using *yucQ* quintuple mutants, which exhibited altered phenotypes due to insufficient auxin levels. These deficiencies could not be compensated for solely by auxin transport from the shoot, highlighting the importance of local auxin biosynthesis in root tissues (Chen et al., 2014).

Local auxin biosynthesis is a key adaptive mechanism that allows plants to generate targeted responses to environmental stimuli (Zhao, 2018). For example, the local production of YUC enzymes plays a critical role in adapting to heat stress. Specifically, *YUC9* is upregulated in *Arabidopsis* under high-temperature conditions (Cao et al., 2019). These findings highlight the importance of localized auxin biosynthesis in environmental responses and offer a promising perspective for further research. Understanding the role of local auxin biosynthesis in stress adaptation could provide critical insights into how plants cope with adverse environmental conditions and may lead to strategies to mitigate these challenges.

1.6. Recombineering lines: a toolset for expression analysis

To study the expression of IAA biosynthesis genes, we used recombineering lines generated using the protocol described by Brumos et al. (2020). Recombineering is a genetic engineering technique that enables the precise modification of large DNA fragments. This method was developed to address the limitations of traditional transformation techniques, which frequently result in the loss of regulatory regions essential for accurate gene expression analysis.

The recombineering process utilizes the homologous recombination machinery of the *Escherichia coli* lambda red phage system to construct large DNA cassettes. These cassettes contain the gene of interest along with its

native regulatory elements, ensuring the preservation of critical upstream and downstream sequences. In our study, the gene of interest was fused to a reporter gene encoding β-glucuronidase (GUS), allowing for precise visualization of gene expression patterns through histochemical staining.

This approach provides a robust tool for studying gene regulation in plants by maintaining the native genomic context of the target gene, offering a more accurate understanding of spatiotemporal expression (Brumos et al., 2020).

Since external stimuli, such as temperature, can modify the expression patterns of auxin biosynthesis genes and, consequently, auxin accumulation, this study aims to define the spatiotemporal expression patterns of auxin-related genes under different temperature conditions (20 °C, 28 °C, 34 °C, and 40 °C) and analyse their differences. This investigation will provide insights into how temperature variations affect auxin dynamics and contribute to the understanding of plant developmental plasticity in response to environmental changes.

2. Objectives

Our research revolves around how environmental factors affect auxin availability in meristematic tissues. The prevalent view in the field is that auxin accumulates in the meristems mainly due to transport. This study aims to examine the role of local auxin biosynthesis in response to increasing temperatures (20 ºC, 28 ºC, 34 ºC, and 40 ºC) and how the temperature-auxin effect shapes root architecture.

To achieve this, we focused on the following specific objectives:

2.1. Phenotyping of the root system architecture

2.1.1. To analyze the impact of different temperatures on root system architecture, specifically quantifying number of lateral roots and primary root growth in WT *Arabidopsis* (Col-0) and auxin biosynthesis mutants (*wei8-1* and *wei8-1 tar2-1*).

2.2. Characterization of auxin response by analyzing *DR5* reporter expression patterns

2.2.1 To determine spatiotemporal dynamics of auxin response in *Arabidopsis* roots under different temperatures.

2.2.2. To investigate the differential regulation of *DR5* activity between 28 ºC and 34 ºC and to determine whether auxin accumulation is induced or repressed under these thermal conditions: thermomorphogenesis *vs* heat stress.

2.3. Characterization of auxin biosynthesis gene expression patterns

2.3.1. To quantify and characterize the expression patterns of key auxin biosynthesis genes (*TAA1/TARs* and *YUCs*) in roots exposed to different temperature conditions, with particular emphasis on identifying induction or repression between 28 ºC and 34 ºC.

2.4. Characterization of auxin catabolism gene expression patterns

2.4.1. To quantify and characterize the expression patterns of auxin catabolism gene *DAO1* in roots exposed to increasing temperature conditions, with particular emphasis on identifying differential expression between 28 ºC and 34 ºC.

2.5. Identification of potential transcription factors regulating local auxin biosynthesis

2.5.1. To analyze available ChIP-seq data for the IPyA pathway genes

2.5.2. To analyze available DAP-seq data for the IPyA pathway genes

3. Material and methods

3.1. Plant material

We utilized *A. thaliana* Col-0 seeds obtained from the laboratory's seed collection. Specifically, recombineering lines of IAA biosynthesis genes involved in the IPA pathway (*TAA1/TARs* and *YUCCAs*) were employed to analyse spatiotemporal expression patterns (Brumos et al., 2020). Additionally, seeds of the single mutant *wei8-1* and double mutant *wei8-1 tar2-1* in the Col-0 background were used for phenotypic assays (Stepanova et al., 2008; Brumos et al., 2018). Furthermore, seeds of the *DAO1p:GUS* line, which reports the expression of a gene involved in IAA catabolism, were used to analyze the activity of this metabolic pathway (Mellor et al., 2016).

3.2. Seed sterilization

To sterilize the seed surfaces, a 50% bleach solution with 0.01% Triton X-100 was applied. A volume of 1.2 mL of this solution was added to each tube containing seeds, which were then incubated for 15 minutes. During this time, the tubes were gently agitated to expose all the seeds equally to the bleach solution and break up any clumps. After incubation, the bleach solution was removed by vacuum aspiration and the seeds were rinsed six times with autoclaved deionized water to fully eliminate any bleach residue. This procedure was performed under a flame to maintain sterile conditions throughout the process. Finally, seeds were stored at 4 °C with 100 µL of autoclaved deionized water per tube during at least three days to induce cold stratification for synchronizing germination.

3.3. Plant growth conditions and physiological assays

Seeds for the temperature assays were sown in 9 mm Petri dishes containing MS medium without sucrose, composed of 4.3 g/L MS salts and 8 g/L agar, adjusted to pH 5.8 with KOH 1M. To ensure precise seed plating, the seeds were resuspended in 0.7% low-melting-point agarose and evenly arranged in rows on the surface of the MS medium using a 200 µL pipette with wide-bore tips.

Generally, germination was performed by incubating the seeds in Petri dishes in an in vitro growth chamber at 23°C under long-day photoperiod conditions (16 hours light/8 hours dark) for 5–7 days. However, to efficiently

and unequivocally identify the *wei8-1* single mutant and the homozygous *wei8-1 tar2-1* double mutants (the infertility of *wei8-1 tar2-1* lines requires to be propagated as sesqui-mutants), the auxin biosynthesis double mutant *wei8-1 tar2-1/+* lines were germinated in darkness on sucrose-free MS medium supplemented with 10 µM 1-aminocyclopropane-1-carboxylic acid (ACC), an ethylene precursor, to induce the triple response. The homozygous *wei8-1 tar2-1* double mutant plants are unable to respond to ethylene and the *wei8-1* single mutant plants display clear phenotypic differences with the double mutant and *Col-0* wild-type.

Once the seedlings had developed, they were either transferred to square plates for phenotypic analyses, such as primary root growth and lateral root number quantifications, or kept in round Petri dishes for studies on gene expression patterns.

3.4. GUS staining and tissue clearing with ClearSee

The GUS staining protocol was performed in accordance with the methodology described by Brumos et al. (2020). Initially, seedlings were collected in tubes containing 90% acetone for tissue fixation and were subsequently stored at -20 °C overnight to preserve cellular integrity and to help remove chlorophyll. The following day, seedlings were transferred to clean tubes containing rinse buffer composed of 50 mM NaPO4 buffer, pH 7.0, 0.5 mM K3Fe(CN)6, and 0.5 mM K4Fe(CN)6, and were washed twice to eliminate any residual acetone which may interfere with subsequent staining.

Then, seedlings were immersed in the staining solution, which consisted of rinse buffer with the GUS enzyme substrate X-Gluc at a final concentration of 1 mg/mL. To facilitate the diffusion of X-Gluc across cellular membranes, dimethyl sulfoxide (DMSO) at a final concentration of 1% v/v was used as solvent of the X-Gluc stock. This enhance the permeabilization of plant tissues. For best penetration of X-Gluc into the plant cells, vacuum infiltration was applied in five cycles of 1-minute each.

The samples were incubated at 37 °C during 16h (unless otherwise stated) to allow for sufficient enzymatic activity, enabling the GUS enzyme to hydrolyse X-Gluc and produce a blue precipitate indicative of GUS expression. Finally, the staining reaction was stopped by adding 96% ethanol to the samples, achieving a final ethanol concentration of 32%, which effectively stops enzymatic activity and preserves the stained tissues for subsequent analysis and imaging.

Following the termination of the GUS staining reaction, seedlings were placed in tubes with ClearSee, a solution essential for tissue clearing and cellular preservation to facilitate deeper imaging and analysis. The ClearSee solution, prepared according to the protocol by Kurihara et al. (2015), consisted of 10% xylitol, 15% sodium deoxycholate, and 25% urea, diluted to a final volume of 100 mL with deionized water. To ensure complete tissue clearing, seedlings were incubated in this solution in darkness for a minimum of 7 days. This prolonged exposure allows ClearSee to thoroughly permeate the tissues, enhancing optical transparency while maintaining cellular integrity for subsequent imaging, analysis and quantification (Serrano-Mislata & Brumos, 2023).

3.5. Microscopy

The expression patterns of the genes of interest in the root system of *DR5* and recombineering lines were analyzed using differential interference contrast (DIC) microscopy. Seedlings were mounted on microscope slides with ClearSee solution to ensure sample preservation and improve image clarity. A Nikon Eclipse Ni microscope was used for image acquisition, equipped with a DS-Fi3 camera. The imaging process was performed using NIS-Elements L imaging software. A 20x objective lens was used for all captures. The imaging parameters were: automatic exposure (AE) at 20 ms, analogue gain at 1.0x, and AE compensation at -0.16 EV. The resolution of the images was configured to 3x8-bit with a final output of 2880x2048 pixels.

3.6. GUS quantification and measure of phenotypic characters

We used the open-source image analysis software FIJI/ImageJ (Rueden et al., 2017) for the quantification of GUS signal intensity, measurement of primary root growth, and count of lateral root number.

To measure GUS intensity in the recombineering lines, we used the images obtained with the Nikon Eclipse Ni microscope. The protocol begins with the inversion of the pixel values of the image, followed by their conversion into an 8-bit format, ensuring that each pixel´s value ranged between 0 and 255. Next, the threshold for each recombineering line was adjusted to align the measurement with the observed staining pattern. Finally, using the "Measure" tool, we quantified parameters such as area (representing the GUS signal area), mean value (the average intensity of the measured pixels), and integrated density (calculated as the product of area and mean GUS staining intensity value).

This methodology was applied to all recombineering lines except for *TAR2*, due to its low signal intensity. For *TAR2*, we followed the protocol described by Kleine-Vehn & Sauer (2017). This method involves converting the blue GUS precipitate into a quantifiable grayscale scale This process included transforming RGB (Red Green Blue) images into the HSB (Hue Saturation Brightness) colour and selecting the saturation channel to measure GUS staining intensity. This approach improved the quantification of GUS staining intensity in the *TAR2* lines. All *TAR2* lines were processed using this quantification method to be able to compare GUS intensities between *TAR2* lines exposed to different treatments.

As stated above, we were interested in comparing GUS staining intensities of the same line among treatments. So, our goal is to identify GUS intensity differences within the same line among treatments and not comparing different recombineering lines among them.

To measure the growth of the primary root, the position of the root tip was marked on the plate every 24 hours. After the final marking, plates were photographed to obtain a picture with all the markings for every single root and perform the measurements. Root length was quantified using the ImageJ "segmented line" tool to trace the root's trajectory each day and record its length. Each root was measured at least three times, and the average of these measurements was calculated to ensure robustness and accuracy. Average values were used for plotting the graphs and subsequent statistical analysis.

To count the number of lateral roots, the ImageJ "cell counter" tool was employed to mark and record the number of lateral roots per seedling.

3.7. Data analysis

Initial data processing, including calculation of basic descriptive statistics (mean, median, and standard deviation), as well as interquartile range (IQR) calculation for outlier identification, was conducted using Microsoft Excel. Boxplot visualizations of auxin biosynthesis gene expression were generated using RStudio. Phenotypic data were plotted and statistically analyzed using GraphPad Prism software. All experiments were performed with a minimum of $n = 3$ biological replicates.

Statistical analyses were performed as follows. Data normality was assessed using the Shapiro-Wilk test with a significance level of $p < 0.05$. For datasets exhibiting a normal distribution, differences between temperature treatments were analyzed using one-way ANOVA followed by Dunnett´s *post hoc* test to determine pairwise differences. Where data did not meet the assumptions of normality, the non-parametric Kruskal-Wallis test was employed. *Post hoc* comparisons were performed using Dunn´s test with Bonferroni correction for multiple comparisons.

4. Results

4.1. Phenotypic parameters in *Arabidopsis* Col-0 roots under different temperature conditions

To determine how temperature affects root development in *A. thaliana* Col-0, seedlings were grown for 7 days under standard environmental conditions (23 ºC, long-day photoperiod) and then exposed to four different temperatures: 20 ºC, 28 ºC, 34 ºC, and 40 ºC for 5 days.

Primary root growth was monitored daily throughout the treatment period (Figure 6C). Quantification and subsequent statistical analysis of the data showed significant differences in primary root growth depending on the temperature and duration of exposure. Seedlings grown at 20 ºC and 28 ºC exhibited consistent root elongation over time, while those exposed to 34 ºC and 40 ºC exhibited a marked reduction in growth starting from the second day. To provide a comprehensive view of these effects, the total primary root growth at the end of the 5-day period was calculated (Figure 6A). Seedlings exposed to temperatures above 34 ºC exhibited a drastic reduction in root length, indicating a severe inhibitory effect of heat stress on root development. The statistical analysis showed that root length of seedlings exposed to 34ºC has a significant difference ($p < 0.0001$) compared to the control (20 ºC) and the thermomorphogenesis condition (28 ºC).

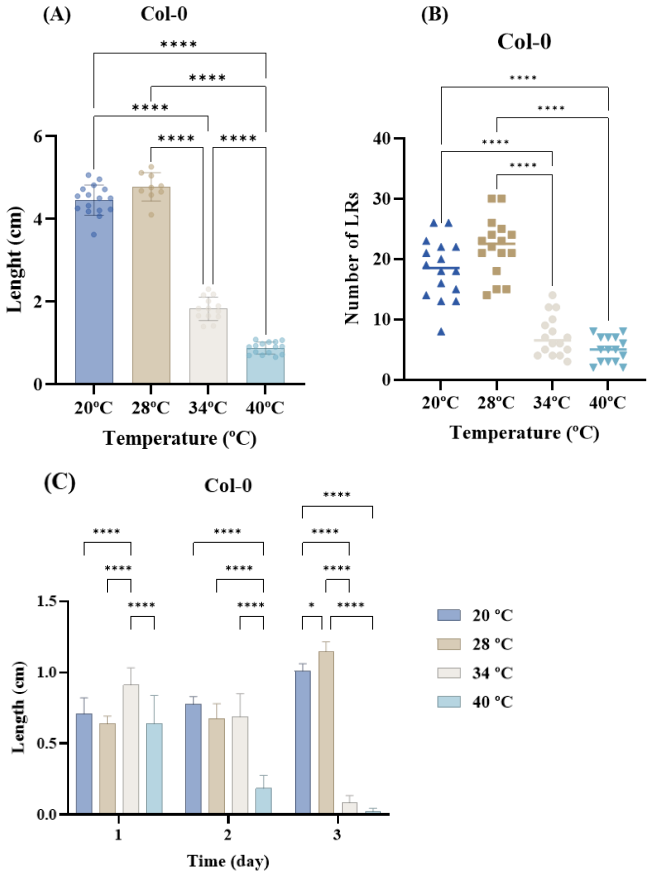

Figure 6. Root phenotypic parameters after 5 days of temperature treatment in Col-0 Arabidopsis seedlings. (A) Growth of primary root after 5 days of being in different temperature conditions **(B)** Number of LRs per seedling at the end of the treatment. **(C)** Growth of primary root the first three days of treatment.

Level of significance: * p<0.05; ** p<0.01; *** p<0.001; **** p < 0.0001

Lateral root (LR) formation was also quantified at the end of the 5-day treatment period (Figure 6B). Significant differences were observed across the temperature conditions. Specifically, a pronounced reduction in the number of LRs was observed at higher temperatures (34 ºC and 40 ºC), aligning with the observed reduction in primary root growth under these conditions. Conversely, at 28 ºC, there was an apparent increase in the number of LRs compared to seedlings grown at 20 ºC, although this increase was not statistically significant. These results suggest that moderately elevated temperatures may enhance certain aspects of root system architecture, provided they remain within a tolerable range.

The statistical analysis further revealed highly significant differences ($p < 0.0001$) across all temperature treatments when compared to the control (20 ºC), emphasizing the strong impact of temperature on root system architecture.

These observations underscore the sensitivity of root development to thermal changes, with optimal root growth and architecture occurring at suboptimal temperatures (28 ºC), whereas higher temperatures (34 ºC and 40 ºC) progressively impair both primary root elongation and lateral root formation.

A temporal analysis of root elongation (Figure 6C) suggests that initial 48 hours of exposure are critical for determining root growth. At 28 ºC, primary root elongation was less pronounced during the initial two days compared to 20 ºC, after which the growth rate stabilized. On the other hand, exposure to 34 ºC and 40 ºC led to a rapid decline in elongation after the first day. These differences were statistically significant ($p < 0.0001$), suggesting a dynamic change in temperature responses over time.

Taken together, these findings suggest that root development is finely tuned to temperature changes, with moderate increases (28 ºC) supporting growth, whereas temperatures of 34 ºC or higher severely impair both primary and lateral root development. The observed phenotypic changes could be linked to temperature-induced disruptions in auxin availability, which plays a key role in regulating root architecture.

In conclusion, root system architecture in *Arabidopsis* is profoundly influenced by temperature, with moderate increases (28 ºC) promoting growth, while higher temperatures (≥ 34 ºC) severely impair root development. These findings provide important insights into the temperature-dependent plasticity of root systems and highlight the potential role of auxin availability in mediating these responses.

To determine whether auxin biosynthesis is required for the root response to elevated temperatures, we conducted an assay using IAA biosynthesis mutants to evaluate whether phenotypic parameters were affected under different temperature conditions.

Primary root length varied significantly among genotypes and across temperatures (Figure 7A). The control genotype (Col-0) exhibits slightly greater primary root growth at 28 °C compared to 20 °C, although the difference is not statistically significant. However, at 34 °C, a trend toward reduced root growth becomes evident, which is even more pronounced in seedlings grown at 40 °C. In contrast, the mutant genotypes *wei8-1* and *wei8-1 tar2-1* display compromised primary root growth.

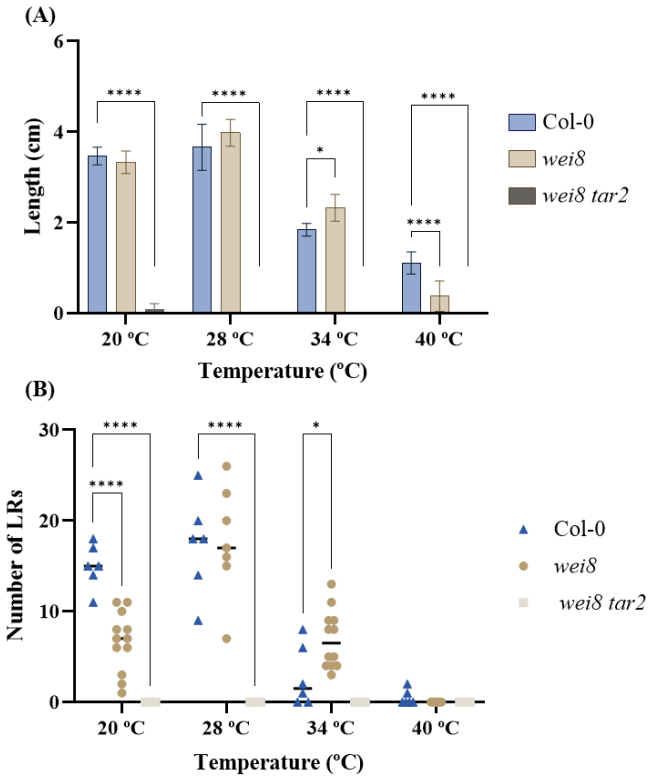

Figure 7. Effect of temperature on root development in *Arabidopsis*. **(A)** Primary root growth in WT (Col-0) and mutant (*wei8-1* and *wei8-1 tar2-1*) seedlings grown at 20 ºC, 28 ºC, 34 ºC, and 40 ºC for 4 days.

(B) Number of LRs under the same conditions. Bars represent mean ±SD. Individual data points are shown. Statistical significance was determined by two-way ANOVA followed by Tukey´s post hoc test. Significant differences relative to the Col-0 control at each temperature are indicated as follows: * $p < 0.05$; ** $p < 0.01$; *** $p < 0.001$; **** $p < 0.0001$. $n = 4 – 12$ biological replicates.

For the single mutant *wei8-1*, root lengths are comparable to those of Col-0 at 20 °C and 28 °C. However, at 34 °C, *wei8-1* exhibits significantly greater root elongation compared to the control ($p < 0.05$). On the other hand, the double mutant *wei8-1 tar2-1* shows impaired root growth across all temperature conditions, highlighting the critical role of auxin in maintaining proper root architecture under elevated temperatures.

The number of lateral roots was also quantified at the end of the temperature treatment (Figure 7B). At 20 °C, Col-0 displayed a significantly higher number of LRs (approximately 15) compared to both *wei8-1* (approximately 8) and *wei8-1 tar2-1* (0). However, at 28 ºC, *wei8-1* exhibit almost the same LRs than Col-0. On the other hand, *wei8-1 tar2-1* does not show formation of LRs, at any temperature tested 28, 34, or 40 ºC.

At 34°C, LR number decreased sharply in all genotypes. *wei8-1* maintained a slightly higher number of LRs compared to Col-0. At 40°C, LR formation was nearly completely inhibited in all genotypes.

4.2. Expression patterns and levels of expression of *DR5* reporter under different temperature conditions

Studies examining phenotypic traits under varying temperature conditions have demonstrated a clear influence of temperature on root system development. These findings highlight the importance of understanding the molecular mechanisms underlying temperature-mediated changes in root architecture, particularly the role of auxin, a key regulator of root development.

To investigate how the spatiotemporal expression patterns of auxin biosynthesis genes are modulated by temperature, *DR5* and recombineering lines were grown at four different temperatures. Seedlings ($n = 6 – 8$ per condition) were harvested at three distinct time points (3, 6, and 24 h) to gain a detailed understanding of the

root meristem's response to temperature over time. Temperature assays were repeated at least three times for each recombineering line.

Fifteen recombineering lines were analyzed. While some biosynthesis genes did not show a visible expression pattern upon GUS staining (Supplemental Figure 1), the auxin reporter *DR5* and the biosynthesis genes *TAA1, TAR2, YUC3, YUC6, YUC7, YUC8*, and *YUC9* exhibited specific temperature-dependent expression patterns.

The expression levels of *DR5:GUS* reporter indicates the levels of auxin response and it is often used as a proxy to measure the accumulation of free auxin in plant tisssues (Ulmasov et al., 1997). GUS staining levels were quantified using ImageJ (Rueden et al., 2017) determining the integrated density. A slight induction of *DR5:GUS* expression levels was observed at 28°C (Figure8). However, at 34°C, a reduction on *DR5* was observed with increasing exposure time. A significant decrease in *DR5* was also evident at 40°C, where, at 24 h, the root morphology was visibly affected by the temperature. These results indicate not only a difference between exposure to distinct temperatures but also a variable response depending on the exposure time. For instance, seedlings exposed to 34°C for 3 or 6 h appeared to display a considerable auxin accumulation. However, this accumulation decreased notably at 24 h. These results suggest that higher temperatures inhibit *DR5* expression and thus, auxin accumulation in the root tip, potentially affecting root growth and development.

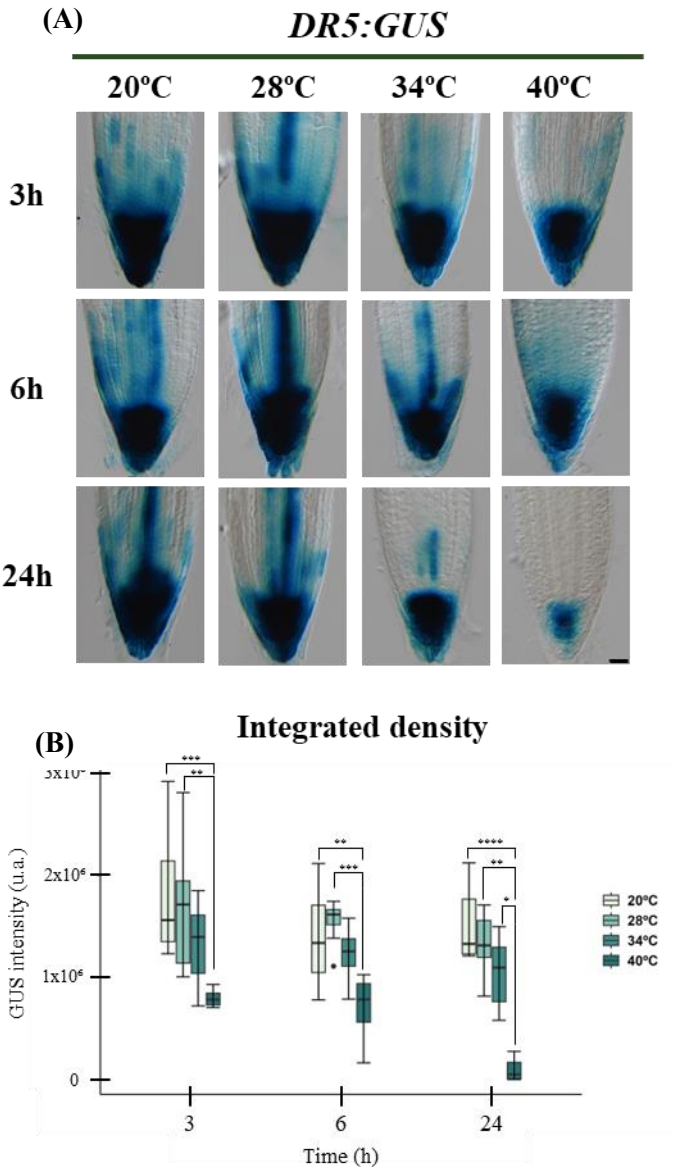

Figure 8. Temperature modulates *DR5:GUS* expression in *Arabidopsis* roots. (A) Representative images of *DR5:GUS* staining in root tips of *Arabidopsis* seedlings growth at 20 ºC, 28 ºC, 34 ºC and 40 ºC for 3, 6, and 24 hours. Scale bar = 20 µm. **(B)** Quantification of *DR5:GUS* activity represented as integrated density. Box-plots show the median, interquartile range, and minimum/maximum values. Statistical significance was determined by Kruskal-Wallis test followed by Dunn test post hoc, and is indicates as follows: * $p<0.05$; ** $p<0.01$; *** $p<0.001$; **** $p < 0.0001$.

To specifically address the differential regulation of *DR5* activity between 28 °C and 34 °C, we focus on determining whether these temperature conditions induce or repress auxin accumulation in root tips.

This assay revealed that *DR5:GUS* expression levels shows differences in auxin accumulation between 28 ºC and 34 ºC, unless there are not statistical significative (Figure 8). On the one hand, the expression level of *DR5* is moderately induced at 28 °C, suggesting that this temperature promotes auxin accumulation in the root tip. On the other hand, a transient induction of *DR5:GUS* activity is observed at 34 °C at 3 h, followed by a reduction at 6 and 24 h. The temporal patterns of *DR5:*GUS expression at 34 ºC indicate a temperature-dependent repression of auxin response.

4.3. Patterns and levels of expression of IAA biosynthesis genes under different temperature conditions

The genes involved in the initial step of the auxin biosynthesis pathway, *TAA1* and *TAR2*, exhibit distinct expression patterns in the root in response to the studied temperature conditions.

Regarding the *TAA1p:GUS* reporter lines (Figure 9A-B), we observed a considerable induction of *TAA1* at 34 °C, particularly at the 3 h time point. However, after 24 h of exposure, roots exposed to 28 °C show a higher expression level than those at 34 °C. This suggests a potentially slower thermomorphogenic response at 28 °C compared to the rapid *TAA1* induction observed at 34°C. The highest expression levels were observed at 28 °C.

The *TAR2p:GUS-TAR2* reporter gene (Figure 9C-D) displayed a different expression pattern compared to *TAA1*. While a slight induction was observed at 28 °C after 3 h, expression levels were generally low across all temperatures and time points. At 34 °C and 40 °C, *TAR2p:GUS-TAR2* expression was barely detectable, especially at the later time points (6 h and 24 h). This suggests that *TAR2* expression is less responsive to temperature changes, particularly at higher temperatures, compared to *TAA1*.

These findings indicate that *TAA1* and *TAR2*, while both involved in the same initial step of auxin biosynthesis, are differentially regulated by temperature. *TAA1* appears to be more sensitive to temperature fluctuations, exhibiting a rapid induction at 34 °C and a sustained expression at 28 °C. In contrast, *TAR2* expression seems to be relatively stable across the tested temperatures, with a small increase at 28 ºC and very low expression at 34 ºC and 40 ºC. *TAR2* expression is generally low but remains unaffected by temperature. This ensures a basal level of IPyA production, allowing *YUCs* to synthesize IAA regardless of temperature fluctuations. In contrast, *TAA1* likely modulates the availability of IPyA, increasing or decreasing its levels to enable *YUCs* to produce more or less IAA depending on environmental temperature changes.

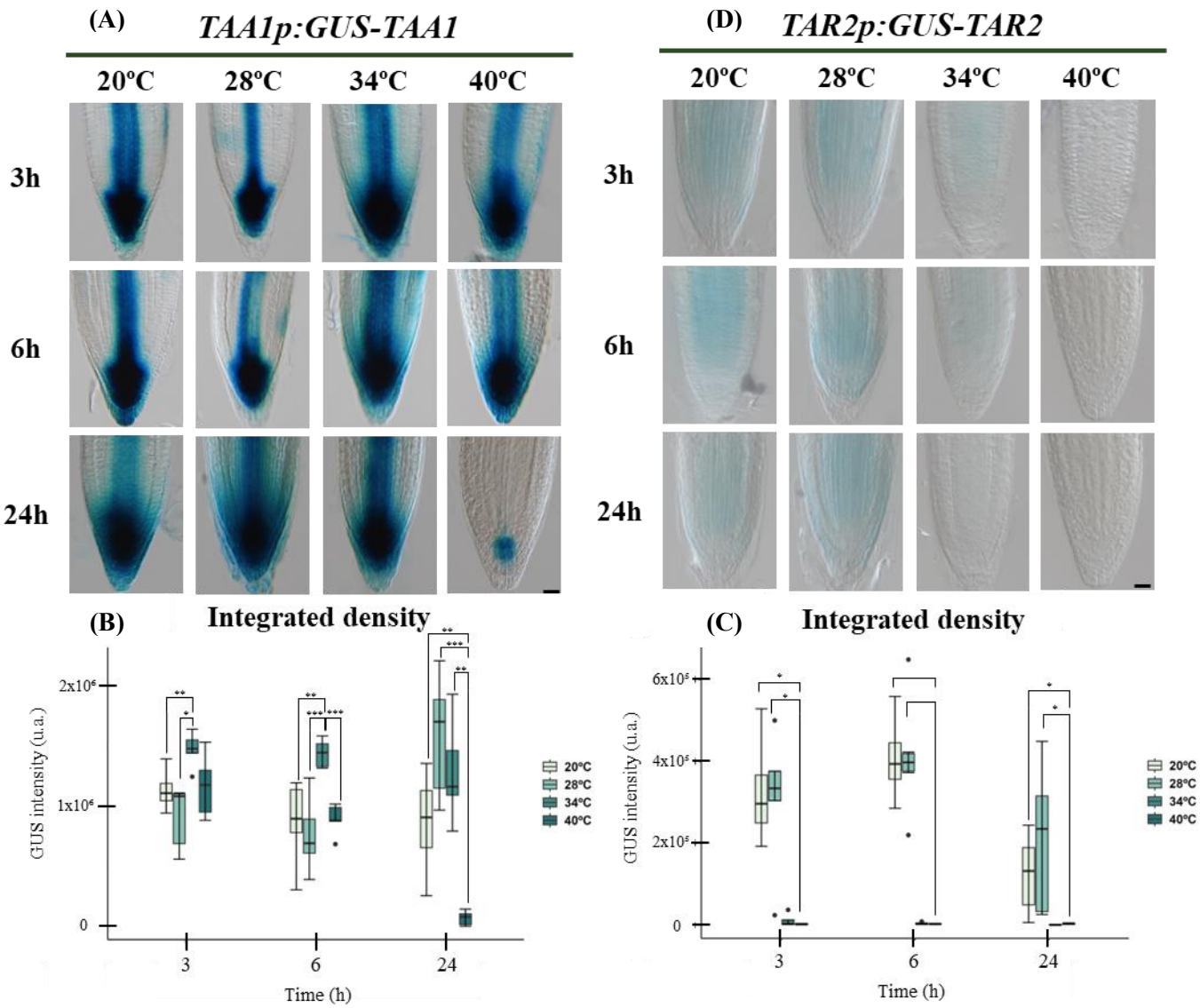

Figure 9. Effect of temperature on *TAA1p:GUS-TAA1* and *TAR2p:GUS-TAR2* expression in *Arabidopsis* roots. (A) Representative images of *TAA1p:GUS-TAA1* staining in root tips of seedlings growth at 20 ºC, 28 ºC, 34 ºC and 40 ºC for 3, 6, and 24 hours. Scale bar = 20 µm. **(B)** Quantification of *TAA1p:GUS-TAA1* activity represented as integrated density. Box-plots show the median, interquartile range, and minimum/maximum values. Statistical significance was determined by one-way ANOVA test followed by Dunnett test post hoc, and is indicates as follows: * p<0.05; ** p<0.01; *** p<0.001; **** p < 0.0001 **(C)** Representative images of *TAR2p:GUS-TAR2* staining in root tips of seedlings growth at 20 ºC, 28 ºC, 34 ºC and 40 ºC for 3, 6, and 24 hours. Scale bar = 20 µm. **(D)** Quantification of *TAR2p:GUS-TAR2* activity represented as integrated density. Box-plots show the median, interquartile range, and minimum/maximum values. Statistical significance was determined by Kruskal-Wallis test followed by Dunn test post hoc, and is indicates as: * p<0.05; ** p<0.01; *** p<0.001; **** p < 0.0001.

Having examined the expression of genes involved in the initial step of auxin biosynthesis, we then analyzed the expression patterns and levels of the *YUC* genes, which catalyse the second step of the IPyA auxin biosynthesis pathway.

The reporter *YUC3p:YUC3-GUS* (Figure 10A-B) showed a distinct expression across the different temperatures and time points. At 20°C and 28°C, *YUC3p:YUC3-GUS* expression is consistently observed throughout the different time point (3 , 6, and 24 h). Nevertheless, at 34°C the expression is initially high at 3 h but decreases significantly by 24 h. At 40°C, *YUC3p:YUC3-GUS* expression is drastically reduced at all time points. Quantification of *YUC3p:YUC3-GUS* activity (Figure 10B) confirms these observations. The highest activity is

seen at 34 °C at the 6h time point. Statistical analysis indicates significant differences in *YUC3p:YUC3-GUS* expression across temperatures, especially at 6h.

Representative images of *YUC6p:YUC6-GUS* staining (Figure 10C) also show temperature-dependent expression. A slight increase can be observed at 6 h for 28 °C. At 34 °C, *YUC6p:YUC6-GUS* expression is initially detected at 3 h but decreases substantially at 6 h and is almost absent at 24 h. At 40 °C, *YUC6p:YUC6-GUS* expression is very low at all time points. Quantification of *YUC6p:YUC6-GUS* activity (Figure 10D) supports these visual observations. The highest activity is observed at 28 °C after 3 h. Statistical analysis reveals significant differences in *YUC6p:YUC6-GUS* expression across temperatures, especially at 3 and 6 h.

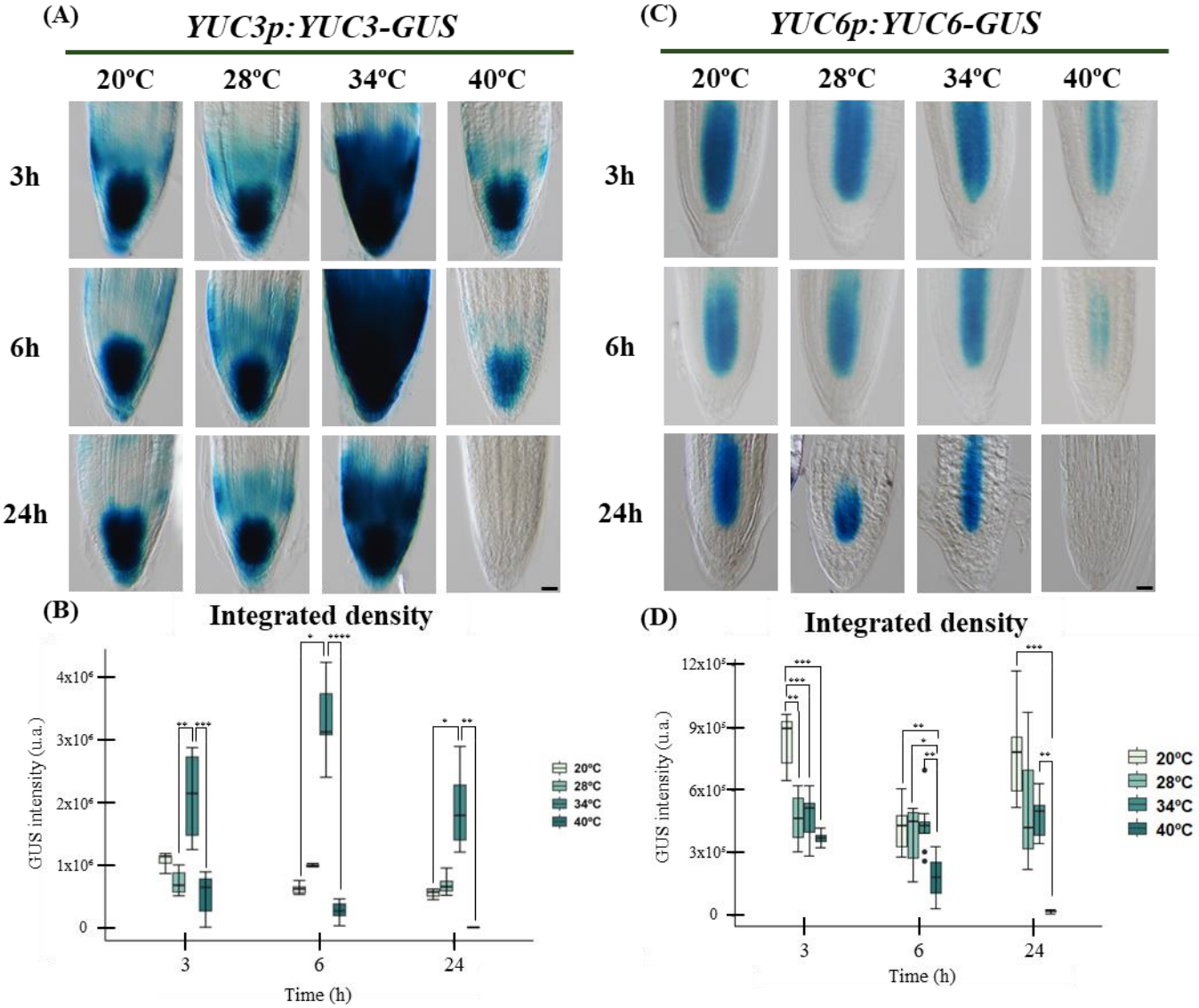

Figure 10. Effect of temperature on *YUC3p:YUC3-GUS* and *YUC6p:YUC6-GUS* expression in *Arabidopsis* roots. (A) Representative images of *YUC3p:YUC3-GUS* staining in root tips of seedlings growth at 20 ºC, 28 ºC, 34 ºC and 40 ºC for 3, 6, and 24 hours. Scale bar = 20 µm. **(B)** Quantification of *YUC3p:YUC3-GUS* activity represented as integrated density. Box-plots show the median, interquartile range, and minimum/maximum values. Statistical significance was determined by Kruskal-Wallis test followed by Dunn test post hoc, and is indicates as follows: * $p<0.05$; ** $p<0.01$; *** $p<0.001$; **** $p < 0.0001$ **(C)** Representative images of *YUC6p:YUC6-GUS* staining in root tips of seedlings growth at 20 ºC, 28 ºC, 34 ºC and 40 ºC for 3, 6, and 24 hours. Scale bar = 20 µm. **(D)** Quantification of *YUC6p:YUC6-GUS* activity represented as integrated density. Box-plots show the median, interquartile range, and minimum/maximum values. Statistical significance was determined by one-way ANOVA test followed by Dunnett test post hoc, and is indicates as: * $p<0.05$; ** $p<0.01$; *** $p<0.001$; **** $p < 0.0001$.

Analysis of representative *YUC7p:YUC7-GUS* staining images (Figure 11A) reveals a clear temperature-dependent expression pattern. Under optimal growth conditions at 20 °C, *YUC7p:YUC7-GUS* expression remains low at every time point analyzed. However, when the temperature was increased to 28°C, we observed a slight increase in *YUC7p:YUC7-GUS* expression, particularly noticeable at 6 h. This increase suggests that 28 °C might be a temperature that modestly favours the expression induction of *YUC7*. Similarly, it seems that the expression of *YUC7* is also induced at 34 ºC. Nevertheless, when the plants are subjected to high temperatures, such as 40 °C, *YUC7p:YUC7-GUS* expression drastically decreases at all time points. This strong expression

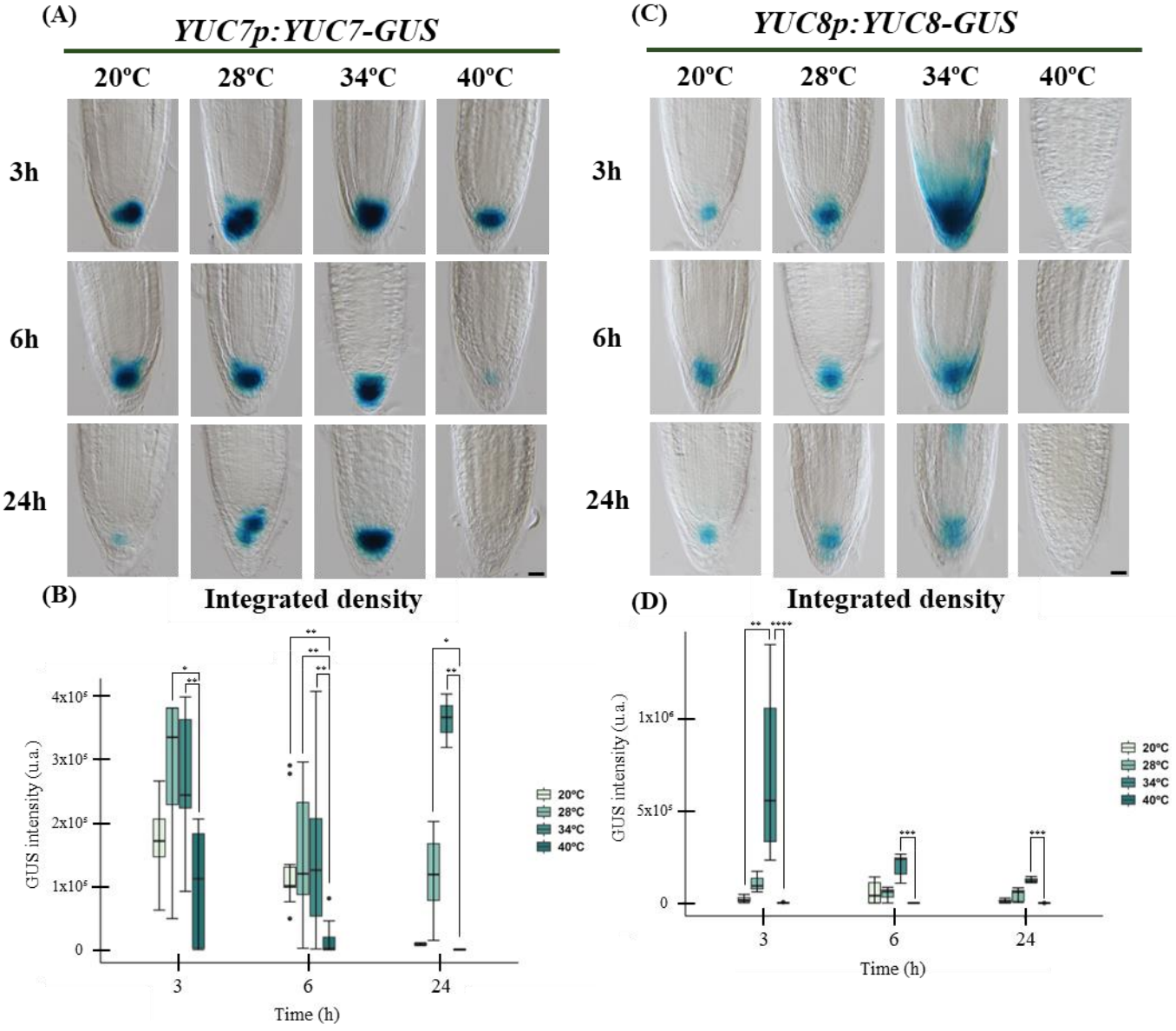

Figure 11. Effect of temperature on *YUC7p:YUC7-GUS* and *YUC8p:YUC8-GUS* expression in *Arabidopsis* roots. (A) Representative images of *YUC7p:YUC7-GUS* staining in root tips of seedlings growth at 20 ºC, 28 ºC, 34 ºC and 40 ºC for 3, 6, and 24 hours. Scale bar = 20 µm. **(B)** Quantification of *YUC7p:YUC7-GUS* activity represented as integrated density. Box-plots show the median, interquartile range, and minimum/maximum values. Statistical significance was determined by Kruskal-Wallis test followed by Dunn test post hoc, and is indicates as follows: * $p<0.05$; ** $p<0.01$; *** $p<0.001$; **** $p < 0.0001$ **(C)** Representative images of *YUC8p:YUC8-GUS* staining in root tips of seedlings growth at 20 ºC, 28 ºC, 34 ºC and 40 ºC for 3, 6, and 24 hours. Scale bar = 20 µm. **(D)** Quantification of *YUC8p:YUC8-GUS* activity represented as integrated density. Box-plots show the median, interquartile range, and minimum/maximum values. Statistical significance was determined by Kruskal-Wallis test followed by Dunn test post hoc, and is indicates as: * $p<0.05$; ** $p<0.01$; *** $p<0.001$; **** $p < 0.0001$.

reduction indicates that high temperatures have an inhibitory effect on *YUC7* expression levels. Quantification of *YUC7p:YUC7-GUS* activity, represented as integrated density (Figure 11B), confirms these visual observations. Statistical analysis supports the existence of a significantly higher activity peak at 34 °C at 24 h, reinforcing the idea that this temperature slightly induces *YUC7* expression.

The *YUC8p:YUC8-GUS* staining images (Figure 11C) show a dynamic expression pattern. At 20 °C, *YUC8p:YUC8-GUS* expression is practically undetectable at all time points. However, upon exposing the roots to 28 °C, we observe a slight expression induction. At 34 ºC during 3 h, the maximum expression of *YUC8* occurs. This induction is very marked, suggesting a rapid and potent response of *YUC8* to this temperature. However, this induction is transient, as the expression considerably decreases at 6 h and is virtually absent at 24 h. This behavior suggests that *YUC8* might be involved in an early response to the 34 °C temperature. *YUC8p:YUC8-GUS* expression remains very low at every time point at 40 ºC. Quantification of *YUC8p:YUC8-GUS* activity (Figure 11D) reinforces these visual observations. Statistical analysis confirms the existence of a very high activity peak at 34 °C at 3 hours, significantly higher than in all other experimental conditions.

Analysis of the *YUC9p:YUC9-GUS* expression patterns revealed distinct temperature-dependent responses. At 3 h, a marked increase in GUS staining intensity was observed at 28 °C and 34 °C compared to the control temperature of 20 °C (Figure 12). This suggests a rapid upregulation of *YUC9* expression under these temperatures. The highest GUS activity at this time point was observed at 34 °C, which was significantly different from the 20 °C treatment, indicating a strong early response to this specific temperature. However, at 40 °C, GUS staining was almost completely absent, suggesting a potential inhibition of *YUC9* expression or activity under severe heat stress.

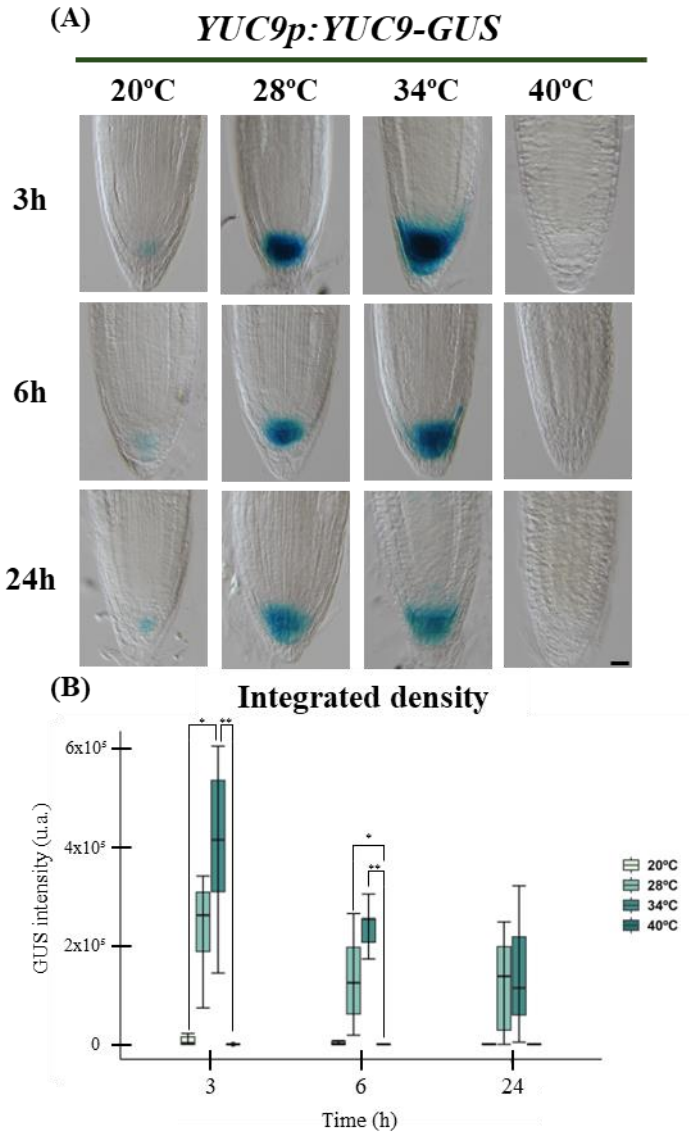

Figure 12. Temperature modulates *YUC9p:YUC9-GUS* expression in *Arabidopsis* roots. (A) Representative images of *YUC9p:YUC9-GUS* staining in root tips of *Arabidopsis* seedlings growth at 20 ºC, 28 ºC, 34 ºC and 40 ºC for 3, 6, and 24 hours. Scale bar = 20 µm. **(B)** Quantification of *YUC9p:YUC9-GUS* activity represented as integrated density. Box-plots show the median, interquartile range, and minimum/maximum values. Statistical significance was determined by Kruskal-Wallis test followed by Dunn test post hoc, and is indicates as follows: * $p<0.05$; ** $p<0.01$; *** $p<0.001$; **** $p < 0.0001$.

At the 6 h time point, the trend observed at 3 h began to shift. While the 28 °C treatment still showed elevated GUS activity compared to 20 °C, the difference was less pronounced. The 34 °C treatment also showed a significant increase in GUS activity compared to the control, but less than in 3h. Notably, the 40 °C treatment remained suppressed, indicating a sustained negative effect of this high temperature on *YUC9* expression.

By 24 h, the differences in GUS staining intensity between the temperature treatments became less distinct. Although the 28 °C and 34 °C treatments still exhibited slightly higher GUS activity compared to 20 °C, these differences were not statistically significant. The 40 °C treatment continued to show low GUS activity. This suggests that the initial temperature-induced changes in *YUC9* expression are transient, with the system potentially adapting or returning towards basal expression levels over time.

In summary, the root expressed auxin biosynthesis genes tend to show an inductive response to increasing temperatures, at least up to 34 ºC, suggesting a potential link between auxin biosynthesis genes upregulation by increasing temperatures. However, the observed auxin response levels do not fully correlate with the expression increase of some of the auxin biosynthesis genes. This discrepancy suggests that additional regulatory mechanisms may play a critical role in modulating auxin responses and/or auxin levels under these temperature conditions in the root system.

4.4. Patterns and levels of expression of IAA catabolism gene under different temperature conditions

One possible explanation for the repression of *DR5* expression levels at 34 ºC, despite the induction of many auxin biosynthesis genes, is the temperature-dependent regulation of auxin catabolism genes. This could explain the reduction of *DR5* expression in the roots at 34 ºC reported above.

To test this hypothesis, we examined the gene *DIOXYGENASE FOR AUXIN OXIDATION 1* (*DAO1*), which encodes an enzyme responsible for the oxidation and subsequent degradation of free auxin (Zhang et al., 2016). Using the reporter line *DAO1p:GUS*, we conducted experiments using the same temperature gradient (20°C, 28°C, 34°C, and 40°C) at three time points (3, 6, and 24 h) as the treatments employed for the IPyA biosynthesis pathway genes.

The *DAO1p:GUS* reporter line displayed rapid saturation of GUS staining, reaching maximum signal intensity within a short incubation time. To prevent oversaturation, the staining reaction was stopped after 30 minutes, unlike the recombineering lines, which were incubated for longer periods (described in 3.4 section).

Despite this adjustment, the high intensity and uniformity of the blue coloration made it difficult to distinguish specific expression patterns in the root tips. To improve visualization, the saturation levels of the images were normalized using ImageJ (Figure 13A). This processing allowed for a clear assessment of potential differences in *DAO1* expression levels across the tested experimental conditions.

Nevertheless, significant statistical differences were not observed beyond the one-way ANOVA analysis at 3 and 6 h (Figure 13B).

Only we observed significant differences at 24 h time point, seedlings exposed to 40 ºC showed a compromised root tip. However, at 34 ºC the expression of *DAO1* seems to be slightly more induced than at 20 ºC or 28 ºC. This suggests a temperature-induced upregulation of *DAO1* expression at 34 ºC. The level of *DAO1* expression induction was not as pronounced as the induction levels observed for the auxin biosynthesis genes that were induced at 34 °C. However, *DAO1* displayed a general expression pattern, showing GUS staining in nearly every root tissue. Whereas the auxin biosynthesis genes displayed more specific or tissue-defined expression patterns.

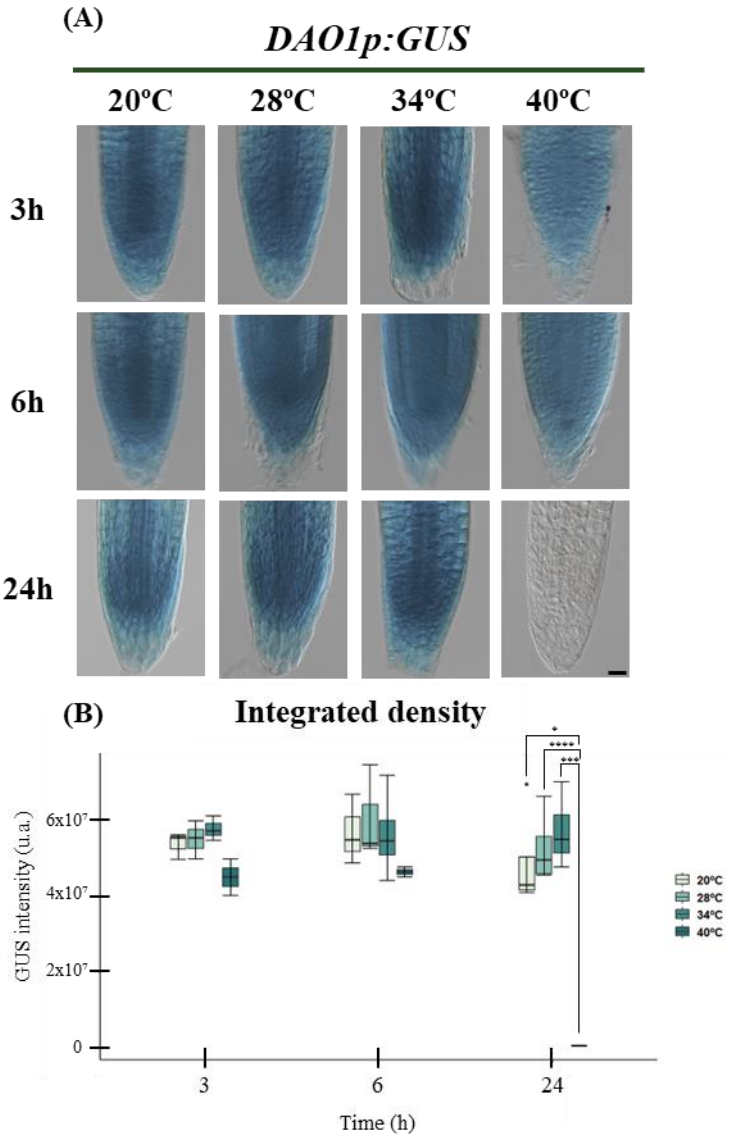

Figure 13. Effect of temperature on *DAO1p:GUS* expression in *Arabidopsis* roots. (A) Representative images of *DAO1p:GUS* staining in root tips of seedlings growth at 20 ºC, 28 ºC, 34 ºC and 40 ºC for 3, 6, and 24 hours. Scale bar = 20 µm. **(B)** Quantification of *DAO1p:GUS* activity represented as integrated density. Box-plots show the median, interquartile range, and minimum/maximum values. Statistical significance was determined by one-way ANOVA test followed by Dunnett test post hoc, and is indicates as follows: * $p<0.05$; ** $p<0.01$; *** $p<0.001$; **** $p < 0.0001$

4.5. *In silico* analysis: Identification of potential transcription factors regulating local auxin biosynthesis

To elucidate the regulation mechanisms of genes in the IPyA biosynthetic pathway, we performed an *in silico* analysis. The objective was to identifying transcription factors (TFs) that may bind to specific regulatory regions of these genes. Relevant data were extracted from publicly available databases to generate a comprehensive overview of potential TF-DNA interactions.

This preliminary analysis serves as an approach for future experimental assays, offering insights into the regulatory networks that may play a key role in modulating the expression of the IPyA biosynthesis pathway genes.

4.5.1. Analyses of available ChIP-seq data for the IPyA pathway genes

To identify candidates TFs, we analyzed Chromatin Immunoprecipitation followed by Sequencing (ChIP-seq) datasets provided by PCBase (http://pcbase.itps.ncku.edu.tw/). This approach showed the *in vivo* interaction between TF and DNA.

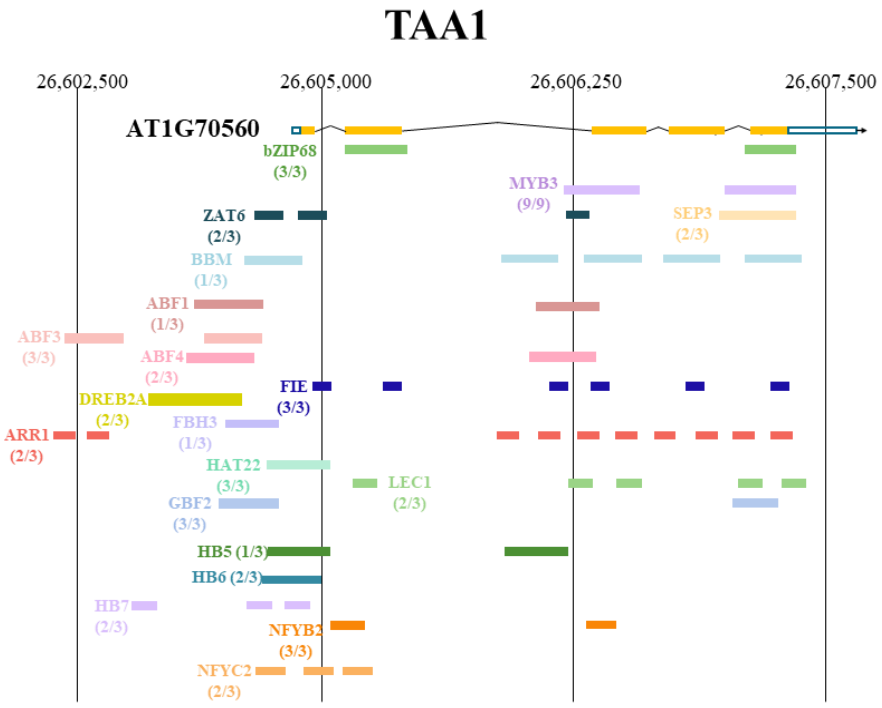

Figure 14. Representation of TFs binding sites associated with *TAA1* (AT1G70560) by ChIP-seq data. *TAA1* is shown in its genomic context (Chr1:26604855...26607652), including 2.8 kb upstream of the transcription start site. *TAA1* orientation is on positive strand (+). Exons are represented as boxes and introns as lines. Coloured boxes represent TFs and their potential binding sites.

TFs associated with *TAA1* belong to 10 distinct TF families with the bZIP (bZIP68, ABFs), HD-ZIP (HBs), MYB (MYB3), bHLH, (FBH3) and ERF (DREB2A) being the most abundant (Figure 14). To obtain more detailed information about the associated TFs, we used the PlantRegMap tool (https://planttfdb.gao-lab.org/tf.php?sp=Ath&did=AT5G04340.1#bind_motif). Among the TFs reported in the ChIP-seq database, ZAT6, DREB2A, and members of the ABF family (ABF1, ABF2, and ABF4) are particularly relevant.

ZAT6 is known to regulate root development, while DREB2A plays a critical role in heat acclimation. Additionally, the ABF family is responsive to abscisic acid (ABA) and water deficit, processes that are often triggered by elevated environmental temperatures. These findings highlight the involvement of diverse TF families in the regulation of *TAA1*, suggesting that some of these TFs could potentially regulate *TAA1* in response to increasing temperatures.

TAR2 showed a lower number of TFs associated with its genomic locus. Among them, MYB3 and EIN6 (=REF6) are the most relevant (Figure 15). MYB3 responds to salt stress, which could be a direct consequence of water deficiency. On the other hand, EIN6 is a TF which participate in ethylene signalling pathway. Thus, the interaction between EIN6 and TAR2 could modulate their expression in response to ethylene, a phytohormone implicated in the suppression of root elongation.

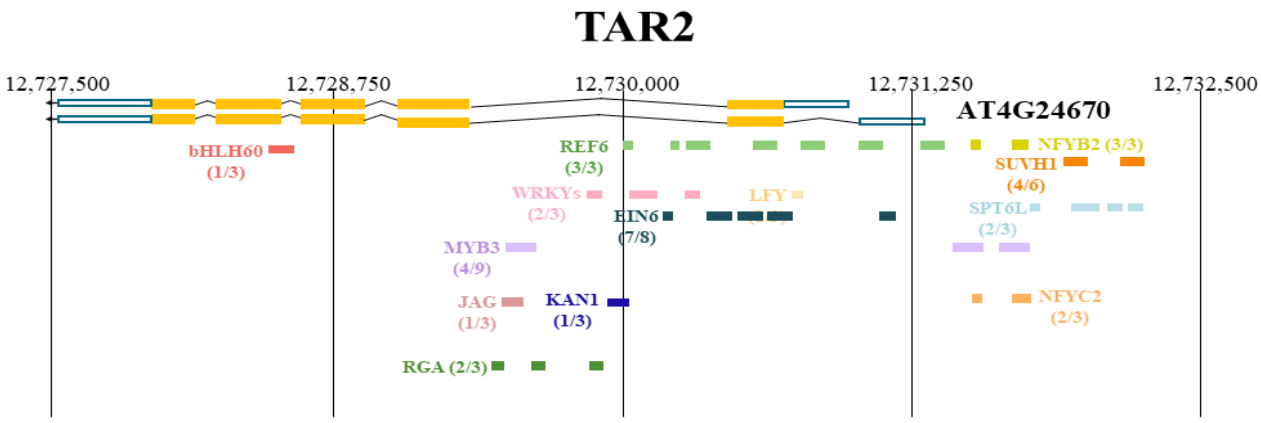

Figure 15. Representation of TFs binding sites associated with *TAR2* (AT4G24670) by ChIP-seq data. *TAR2* is shown in its genomic context (Chr4:12727531…12731331), including 3.8 kb upstream of the transcription start site. *TAR2* orientation is on negative strand (-). Exons are represented as boxes and introns as lines. Coloured boxes represent TFs and their potential binding sites.

In *YUC3*, the association with transcription factors (TFs) occurs throughout the entire genomic region, with the highest number of interactions concentrated in the promoter region (Figure 16). The previously mentioned TFs (EIN6, ZAT6, and members of the HD-ZIP family) show also interaction with *YUC3*. These TFs are able to bind *TAA1*/*TAR2* and *YUC3*, representative members of both steps of the IPyA biosynthesis pathway. These observations suggest that this group of TFs could be directly regulating local auxin production in the specific cell types where they are expressed. Additional TFs bind *YUC3*, the involvement of WRKY33 and MYB44 is particularly notable. WRKY33 is associated with the cellular response to heat acclimation, while MYB44 is characterized as a TF involved in auxin response.

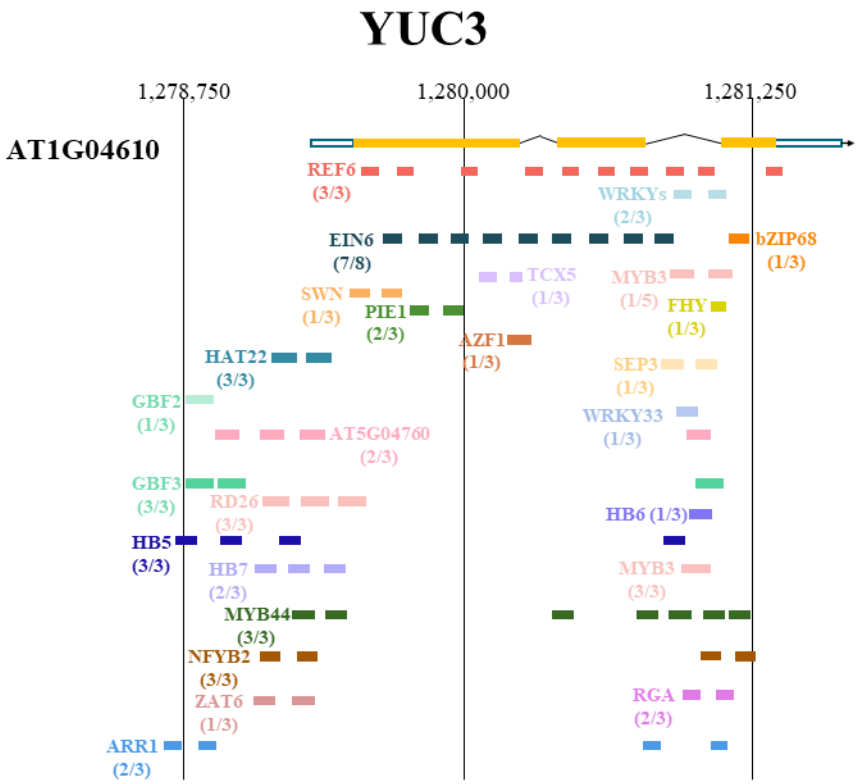

Figure 16. Representation of TFs binding sites associated with *YUC3* (AT1G04610) by ChIP-seq data. *YUC3* is shown in its genomic context (Chr1:1279351...1281618), including 2.3 kb upstream of the transcription start site. *YUC3* orientation is on positive strand (+). Exons are represented as boxes and introns as lines. Coloured boxes represent TFs and their potential binding sites.

In *YUC6*, the associations between TFs and DNA are observed throughout the entire genomic region (Figure 17). Notably, *YUC6* interacts with DREB2A, members of the MYB family, as well as HB5 and HB7 from the HD-ZIP family. Additionally, there is evidence of an association with HON5, a TF involved in the response to reactive oxygen species, which are commonly generated under heat stress conditions.

YUC7 exhibits the fewest interactions with TFs (Figure 18). In this case, only interactions with EIN6 (=REF6) and BBM have been detected.

On the other hand, *YUC8* shows the highest number of TF binding events in its promoter region, with representation from more than 10 different TF families (Figure 19). Among these families, certain TFs stand out as unique to this gene within the IPyA pathway. Examples include ANAC032, ANAC102, PIF4, and PIF5, which are not found associated with other genes in the pathway. Specifically, PIF4 and PIF5 are involved in the regulation of the auxin biosynthesis process and signalling pathways. Some TFs involved in the regulation of *TAA1* also appear in the *YUC8* dataset, including members of the ABF family, HAT22, ZAT6, ARR1, and HD-ZIP family (HB5, HB6, HB7). Additionally, some TFs are associated with both *YUC8* and *TAR2*, such as EIN6, bHLH60, and NFYB2. This suggest that a single TF could regulate IAA production by controlling the expression levels of biosynthesis genes in both steps of the route.

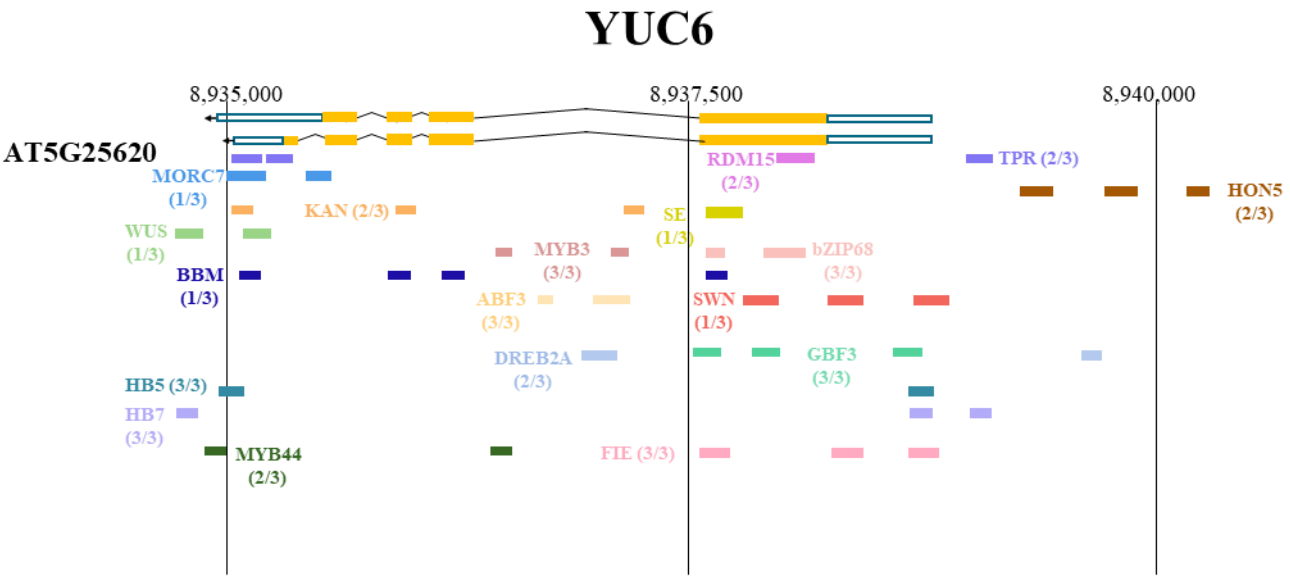

Figure 17. Representation of TFs binding sites associated with *YUC6* (AT5G25620) by ChIP-seq data. *YUC6* is shown in its genomic context (Chr5:8934941...8938768), including 3.8 kb upstream of the transcription start site. *YUC6* orientation is on negative strand (-). Exons are represented as boxes and introns as lines. Coloured boxes represent TFs and their potential binding sites.

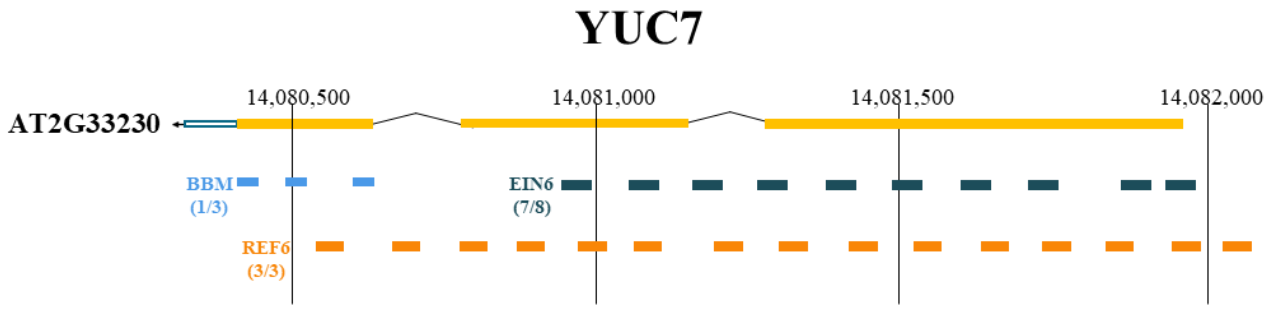

Figure 18. Representation of TFs binding sites associated with *YUC7* (AT2G33230) by ChIP-seq data. *YUC7* is shown in its genomic context (Chr2:14080319...14081971), including 1.7 kb upstream of the transcription start site. *YUC7* orientation is on negative strand (-). Exons are represented as boxes and introns as lines. Coloured boxes represent TFs and their potential binding sites.

Finally, TFs predominantly bind to *YUC9* in its promoter region (Figure 20). Among the TFs interacting with *YUC9*, notable examples include ZAT6, HY5, and MYC2. HY5 belongs to the bZIP TF family and is responsive to varying light intensities. In contrast, MYC2 is a bHLH TF whose activity is associated with desiccation conditions. Most of TFs associated with *YU9* are also related to *TAA1/TAR2*, such as members of HD-ZIP (HB5, HB7) family, ZAT6, ARR1 or MYB3, suggesting that could be involved in regulation of IAA production in cells which express both genes simultaneously.

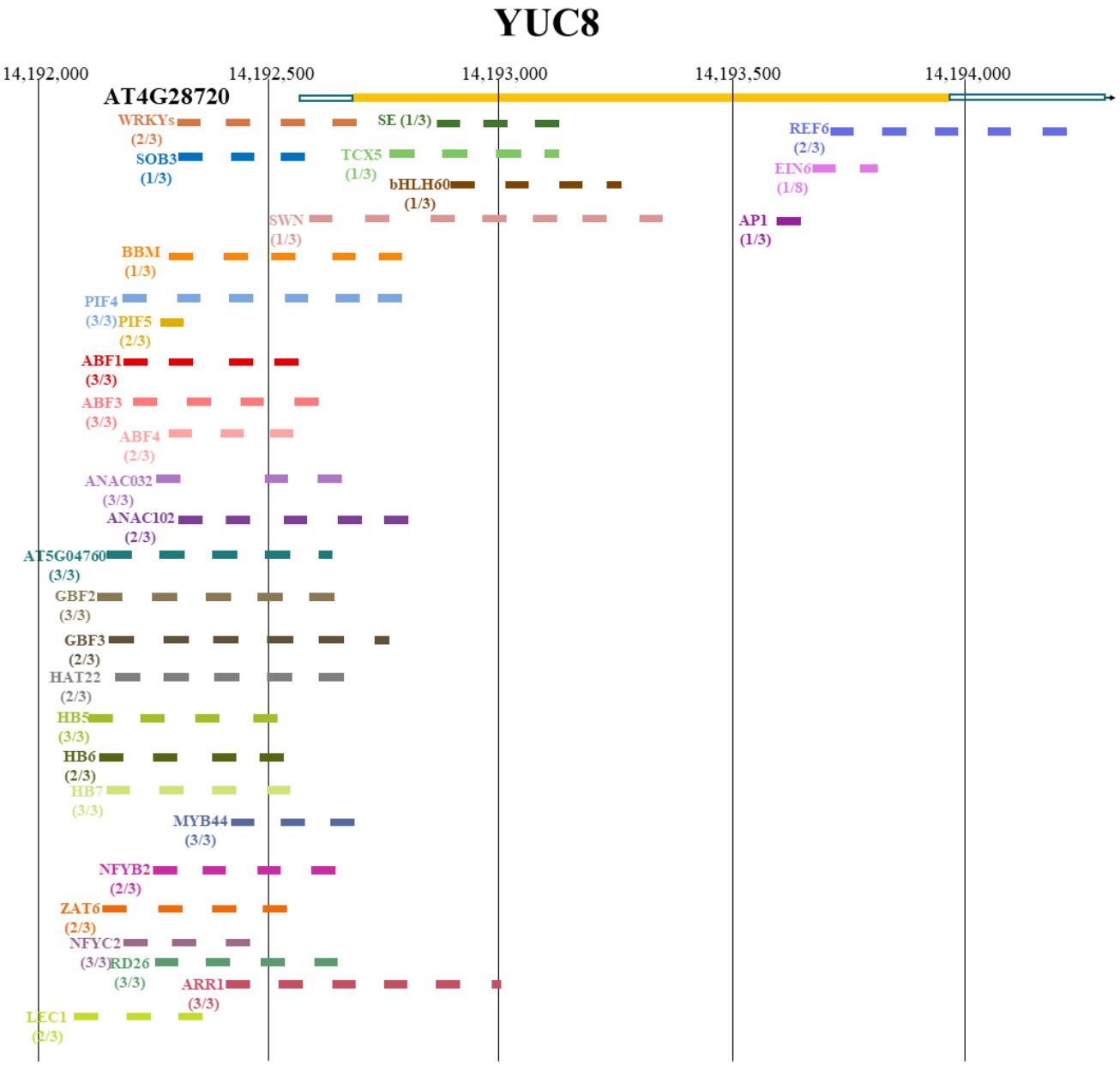

Figure 19. Representation of TFs binding sites associated with *YUC8* (AT4G28720) by ChIP-seq data. *YUC8* is shown in its genomic context (Chr4:14192569…14194302), including 1.7 kb upstream of the transcription start site. *YUC8* orientation is on positive strand (+). Exons are represented as boxes and introns as lines. Coloured boxes represent TFs and their potential binding sites.

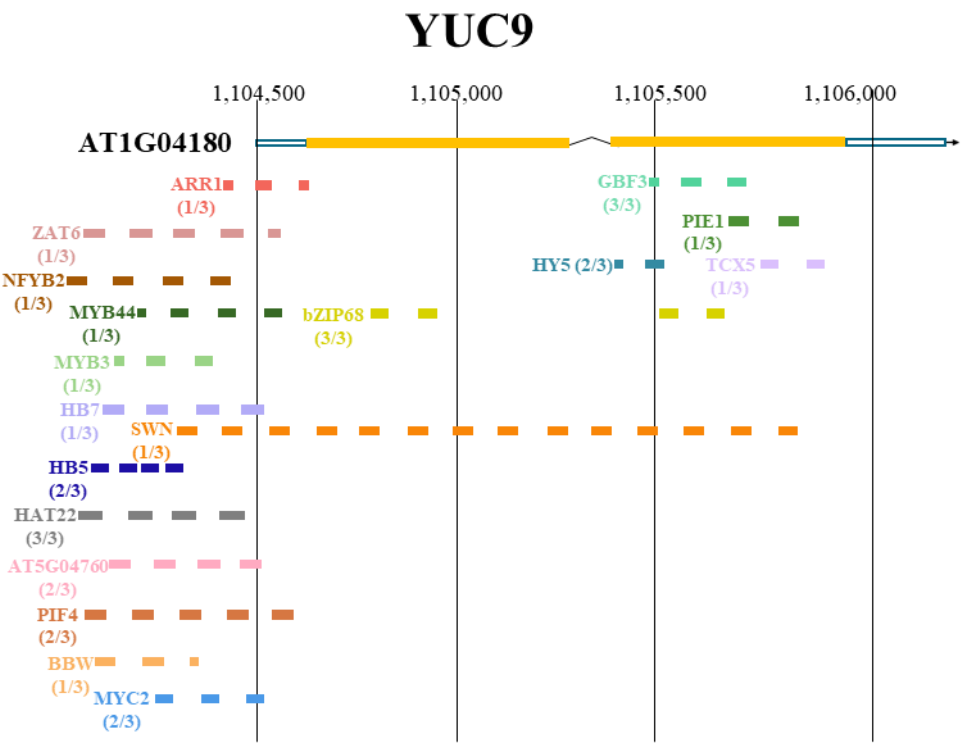

Figure 20. Representation of TFs binding sites associated with *YUC9* (AT1G04180) by ChIP-seq data. *YUC9* is shown in its genomic context (Chr1:1104493...1106241) including 1.8 kb upstream of the transcription start site. *YUC9* orientation is on positive strand (+). Exons are represented as boxes and introns as lines. Coloured boxes represent TFs and their potential binding sites.

4.5.2. Analyses of available DAP-seq data for the IPyA pathway genes

To identify TF binding regions in the genes of the IPyA pathway, we also analyzed DNA Affinity Purification sequencing (DAP-seq) information publicly available. For these analyses, we used the database provided by the published DAP-seq models for *A. thaliana* (http://neomorph.salk.edu/aj2/pages/hchen/dap_ath_pub_models.php). This method enabled us to uncover in vitro interactions between TFs and DNA.

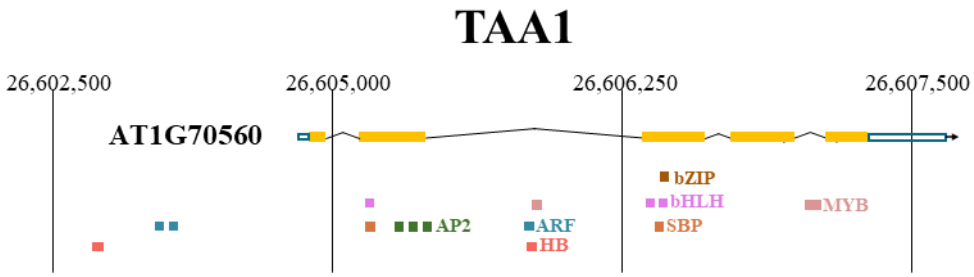

Figure 21. Representation of TFs binding sites associated with *TAA1* (AT1G70560) by DAP-seq data. *TAA1* is shown in its genomic context (Chr1:26604855...26607652), including 2.8 kb upstream of the transcription start site. *TAA1* orientation is on positive strand (+). Exons are represented as boxes and introns as lines. Coloured boxes represent families of TFs and their potential binding sites.

For the DAP-seq data analysis, we select the families of TFs that bind with the IPyA pathway genes. The TFs associated with *TAA1* were predominantly of the bZIP, bHLH, HB and MYB families (Figure 22). Additionally, DAP-seq data also suggested the interactions with ARF and SBP. Nevertheless, there are coincident TFs in both ChIP-seq and DAP-seq datasets, such as bZIP and MYB families, highlighting consistent interactions between this TFs and *TAA1*.

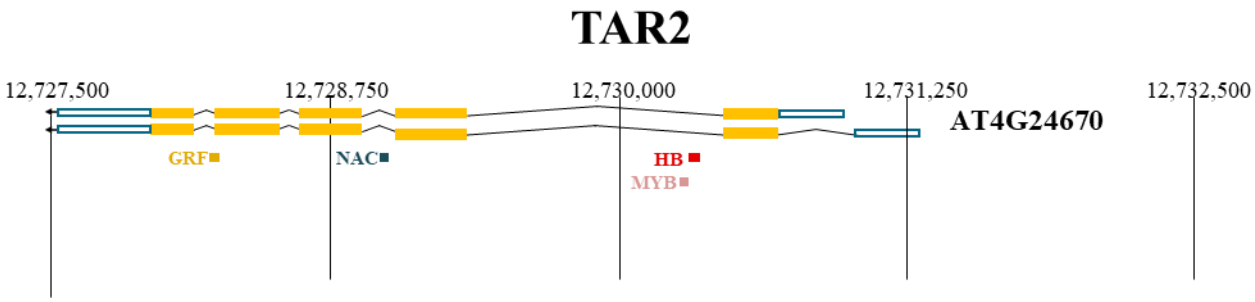

Figure 22. Representation of TFs binding sites associated with *TAR2* (AT4G24670) by DAP-seq data. *TAR2* is shown in its genomic context (Chr4:12727531…12731331), including 3.8 kb upstream of the transcription start site. *TAR2* orientation is on negative strand (-). Exons are represented as boxes and introns as lines. Coloured boxes represent families of TFs and their potential binding sites.

TAR2 binds with other TFs families, in comparison to the ChIP-seq data. For DAP-seq, there are interactions described with GRF, NAC and HB families, that were not being reported in the ChIP-seq. Only MYB appears in both analyses, indicating limited overlap for *TAR2* between both datasets.

Regarding *YUC3*, we identified TFs of same families in both datasets, such as HD-ZIP family (Figure 23). Specifically, HB-related TFs were reported in ChIP-seq and DAP-seq analyses. Additionally, new TFs were reported in DAP-seq. Some examples are REM19, which responds to cold stress, or LBD2, which function is related to root development.

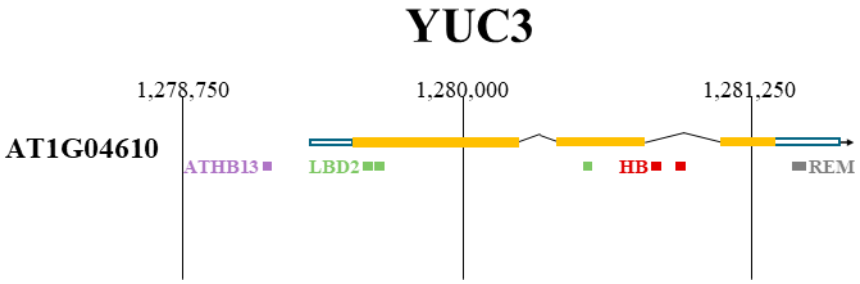

Figure 23. Representation of TFs binding sites associated with *YUC3* (AT1G04610) by DAP-seq data. *YUC3* is shown in its genomic context (Chr1:1279351...1281618), including 2.3 kb upstream of the transcription start site. *YUC3* orientation is on positive strand (+). Exons are represented as boxes and introns as lines. Coloured boxes represent families of TFs and their potential binding sites.

In *YUC6*, most TFs are binding in the promotor region, such as NAC family (Figure 24). TFs from bZIP and MYB families were found to overlap between ChIP-seq and DAP-seq, supporting their potential role in regulating this gene.

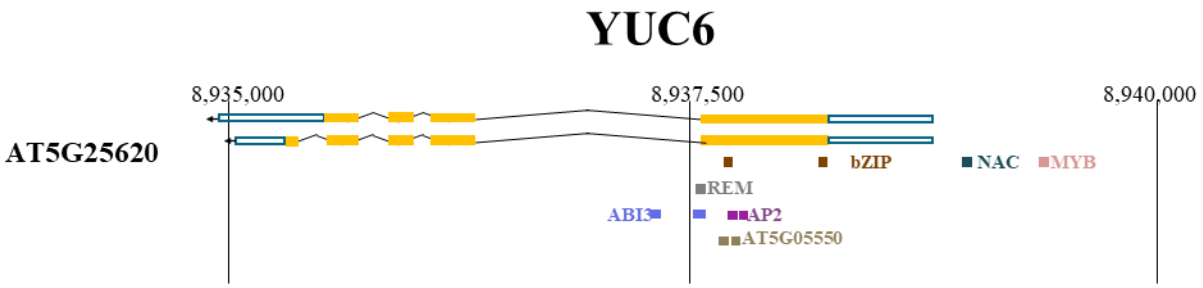

Figure 24. Representation of TFs binding sites associated with *YUC6* (AT5G25620) by DAP-seq data. *YUC6* is shown in its genomic context (Chr5:8934941...8938768), including 3.8 kb upstream of the transcription start site. *YUC6* orientation is on negative strand (-). Exons are represented as boxes and introns as lines. Coloured boxes represent families of TFs and their potential binding sites.

On the other hand, *YUC7* only had AP2 family in common in both analyses. Furthermore, DAP-seq analysis reported the majority of interactions between TFs and *YUC7* near to promoter region, while ChIP-seq analysis showed possible interactions across the entire genomic region. Additionally, DAP-seq provided interactions with new TFs that do not appear on ChIP-seq analysis. Some examples are HB-related, NAC or LBD families (Figure 25).

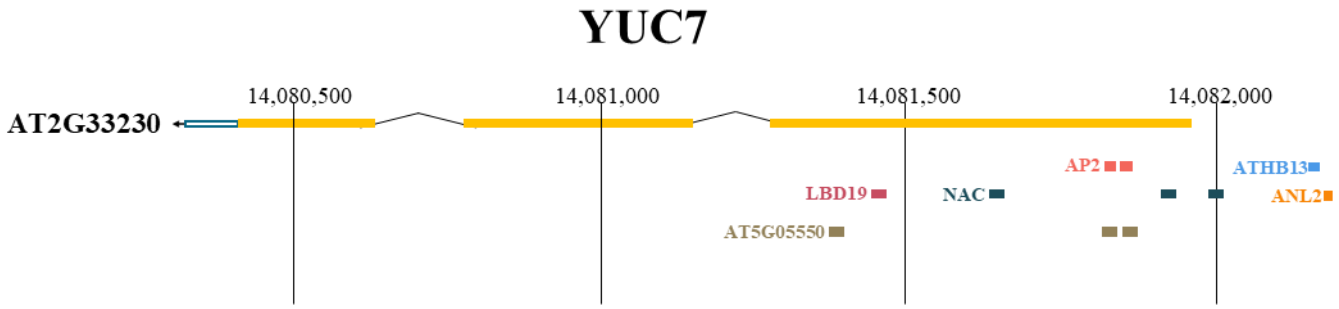

Figure 25. Representation of TFs binding sites associated with *YUC7* (AT2G33230) by DAP-seq data. *YUC7* is shown in its genomic context (Chr2:14080319...14081971), including 1.7 kb upstream of the transcription start site. *YUC7* orientation is on negative strand (-). Exons are represented as boxes and introns as lines. Coloured boxes represent families of TFs and their potential binding sites.

In *YUC8*, TFs binds across all the genomic region (Figure 26), with the presence of bZIP, HSF, bHLH or AP2 families. Several families, including bZIP and bHLH, were identified in both ChIP-seq and DAP-seq datasets. *YUC8* exhibits the highest number of TFs identified in both ChIP-seq and DAP-seq datasets. The presence of same TFs families in both analyses indicates a higher level of consistency in the interactions between *YUC8* and TFs.

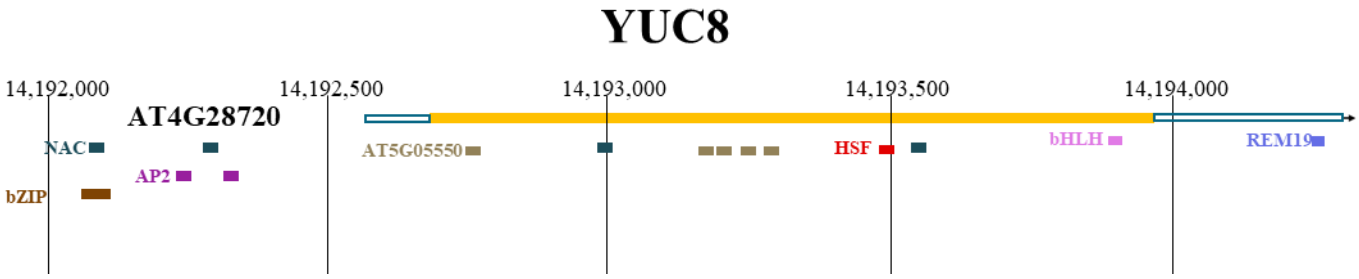

Figure 26. Representation of TFs binding sites associated with *YUC8* (AT4G28720) by DAP-seq data. *YUC8* is shown in its genomic context (Chr4:14192569…14194302), including 1.7 kb upstream of the transcription start site. *YUC8* orientation is on positive strand (+). Exons are represented as boxes and introns as lines. Coloured boxes represent families of TFs and their potential binding sites.

Finally, for *YUC9*, ZAT6 was consistently identified in both ChIP-seq and DAP-seq, indicating a shared interaction with this gene across methodologies (Figure 27). Additionally, DAP-seq provides information about other TFs that binds to *YUC9*. Some examples are BES1, ARR2 or CAMPTA1.

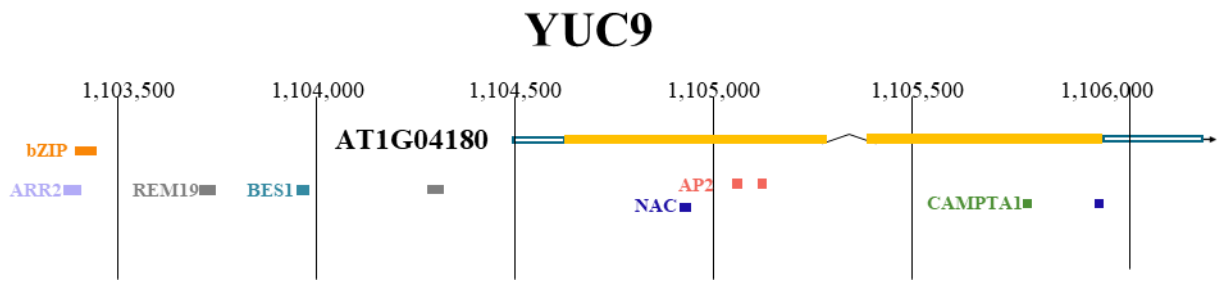

Figure 27. Representation of TFs binding sites associated with *YUC9* (AT1G04180) by DAP-seq data. *YUC9* is shown in its genomic context (Chr1:1104493...1106241) including 1.8 kb upstream of the transcription start site. *YUC9* orientation is on positive strand (+). Exons are represented as boxes and introns as lines. Coloured boxes represent families of TFs and their potential binding sites.

Using the collected data, we can identify potential TFs candidates that could probably regulate auxin biosynthesis genes. These analyses provide a foundation for further exploring the molecular mechanisms underlying temperature responses by analyzing changes in the expression of these TFs under different thermal conditions.

5. Discussion

5.1. Phenotypic effect of temperature on root architecture in *Arabidopsis*

Our data suggested that the phenotypic parameters quantified in wild-type *Arabidopsis* Col-0 roots are significantly influenced by the increasing temperature conditions used in our assays, compared to the 20 °C control temperature.

At 28 °C, we observed a slight increase in primary root length (Figure 6A) as well as in the number of lateral roots (Figure 6B), although these differences were not statistically significant. However, previous studies have reported a significant elongation of the primary root at 28 °C compared to 20 °C after 12 days of growth (Ai et al., 2023). The lack of statistical significance in our study may be attributed to the shorter exposure time, as the enhanced root growth observed by Ai et al. (2023) became evident after six days of exposure to 28 °C. In our study, the effects of temperature on root phenotypes were assessed over a 5-day period, during which we observed the most pronounced increase in root length on the third day of exposure to 28 °C. Notably, root growth during the first two days of exposure was similar to that at 20 °C (Figure 6C). These observations support the hypothesis that root responses to thermomorphogenetic temperatures may be less pronounced during the initial days of exposure.

Seedlings exposed to 34 °C showed a clear reduction in root elongation after 5 days of treatment (Figure 6A). Additionally, the number of lateral roots was significantly reduced (Figure 6B). These results are consistent with similar experiments reported in the literature, which show a marked decrease in primary root length and lateral root numbers in both *Arabidopsis* and tomato seedlings (González-García et al., 2023).

At 40 °C, seedlings exhibited severe root developmental defects after the second day of treatment. Primary root growth was nearly arrested after 5 days of exposure (Figure 6C), and lateral root formation was completely inhibited. Interestingly, during the first day of exposure to 40 °C, primary root growth was comparable to that observed in seedlings grown at 20 °C. This suggests that roots may initially remain a steady elongation rate in response to heat stress, potentially as a strategy to seek cooler soil depths (Ai et al., 2023). However, as high temperatures persist, root growth stops entirely. Thus, our results indicate that at 40 °C, root development is severely impaired, which has a profound impact on seedling survival.

Differences in root phenotypic parameters were also quantified in the mutant genotypes *wei8-1* and *wei8-1 tar2-1*.

For the single mutant *wei8-1*, root growth was comparable to Col-0 control at 20 °C and 28 °C (Figure 7A). This observation is consistent with the findings of Stepanova et al. (2008), where multiple experiments with this single mutant showed no significant differences in root architecture compared to Col-0 seedlings. However, at 34 °C, *wei8-1* exhibited a significantly longer primary root than Col-0 ($p < 0.05$), suggesting that *TAA1* induction in WT seedlings may inhibit primary root growth under high temperatures. Despite this difference, primary root

elongation in both genotypes was reduced at 34 °C compared to the control temperature of 20 °C, consistent with previous observations (Figure 6A; Figure 7A).

The number of lateral roots in *wei8-1* was also affected by temperature. At 20 °C, *wei8-1* produced a significantly fewer number of lateral roots compared to Col-0. However, the number of lateral roots increased substantially in *wei8-1* seedlings exposed to 28 °C. At 34 °C, the number of LRs in *wei8-1* was lower than at 20 °C and 28 °C but still significantly higher than in Col-0 ($p < 0.05$) at 34 °C.

The most pronounced phenotypic effects were observed in the double mutant *wei8-1 tar2-1*, which showed a complete absence of root growth and no lateral root formation across every temperature. This severe root phenotype has been previously documented (Stepanova et al., 2008), highlighting the essential role of TAA1 and TAR2 in root development (Brumos et al., 2018).

5.2. Expression level of *DR5* reporter gene on *Arabidopsis* roots depends on temperature

The results reveal temperature-dependent variations in the expression levels of the *DR5:GUS* reporter line in the root meristem of *Arabidopsis* (Figure 8).

As previously mentioned, a slight induction of *DR5* was observed at 28 °C compared to 20 °C, which was maintained across every time points. Although not statistically significant in our study, other research, such as Ai et al. (2023), reported a higher level of *DR5:GFP* expression at 28 °C. This suggests an increase in auxin accumulation in the root under this condition. This correlates with the enhanced root growth observed in our study, indicating that auxin plays a key role in thermomorphogenic response in roots. Additionally, seedlings were exposed to 28 ºC for 5 days. That could be a reason that we do not report significant differences between 20 ºC and 28 ºC, because our maximum time of exposure were 24 h.

At 34 °C, *DR5* expression pattern became more dynamic. After 3 h of exposure, *DR5* expression resembled basal levels (20 °C). However, staining intensity decreased at subsequent time points (6 and 24 h), indicating that free auxin accumulation in the root was inhibited at 34 ºC.

A similar trend was observed at 40 °C, but starting at lower GUS staining intensity levels than in other temperatures tested. *DR5* expression was strongly inhibited across all time points at 40 ºC. The GUS staining levels at 40ºC are consistent with all the phenotypic parameters quantified at this high temperature (Figure 6). At 34 °C, a significant decrease in primary root growth and lateral root number was observed, likely due impaired auxin accumulation. The same trend was observed at 40 ºC, but the effect was more severe due to the higher thermal stress. Moreover, the similarity in *DR5* expression levels at 3 and 6 h across all temperatures explains the results in Figure 6C, where primary roots grew similarly during the first day of temperature treatment.

When comparing *DR5* expression levels between 28 ºC and 34 ºC, we conclude that 28 ºC induced *DR5* expression, while 34 ºC tends to repress it.

The observed differential response to temperature reflects distinct molecular mechanisms modulating auxin homeostasis under thermogenesis condition (28 ºC) and heat stress (34 ºC). These results underscore the role of temperature in modulating auxin accumulation and its downstream effects on root development. This could correlate with the observed phenotypic parameters. At 28 ºC, *Arabidopsis* primary root displayed more elongation than at 34 ºC.

This difference likely reflects distinct molecular mechanisms regulating auxin homeostasis under thermomorphogenic versus heat stress conditions. However, further detailed studies are necessary to confirm this hypothesis.

5.3. Dynamic changes in IPyA pathway genes patterns and level expression in response to increasing temperature in *Arabidopsis* roots

In these assays of response to increasing temperature of auxin biosynthesis genes, we observed general modifications in expression patterns and levels that varied depending on the analyzed genes, the temperature applied, and the duration of exposure.

The genes of the IPyA pathway first-step expressed in roots (*TAA1/TAR2*) showed distinct responses to temperature (Figure 9). On the one hand, *TAA1* exhibited an increasing induction in expression levels up to 34 ºC. Moreover, *TAA1* expression pattern was observed in the root meristem and provasculature tissue. On the other hand, *TAR2* shows a slight induction at 28 ºC but displayed a minimal expression at 34 ºC, with much lower levels compared to *TAA1*. The expression pattern of *TAR2* was more uniform throughout the root tip at different temperatures. This suggests that *TAR2* expression levels remain invariable maintaining an IPyA production basal level. Whereas, *TAA1* is more influenced by environmental changes in temperature. Therefore, *TAA1* likely plays a more relevant role in modifying the production of IPyA in response to external temperature stimuli in this first step of the IPyA auxin biosynthesis pathway.

The *YUC* genes expressed in roots (*YUC3/YUC6/YUC7/YUC8/YUC9*) also adjusted their expression levels in response to temperature. Except for *YUC6*, all genes involved in this second step of the IPyA biosynthesis pathway are induced at 34 ºC. However, their temporal expression trends are different. In the case of *YUC3,* the induction of expression levels is very evident, reaching maximum levels at 6 hours of exposure to 34°C (Figure 10). With the *YUC7p:YUC7-GUS* reporter line, we also observed a higher level of expression at 34°C (Figure 11A-B), although its expression pattern is much more restricted than that observed in *YUC3*. On the other hand, *YUC8* and *YUC9* exhibited an initial induction at 34 ºC during the first 3 hours of exposure, which gradually declined over time (Figure 11C-D; Figure 12).

Interestingly, the expression pattern of *YUC8* at 34 ºC changed dynamically over time (Figure 11C-D). At the 3 h time point, expression was strongly localized in the meristematic zone, but by 6 h, it became weaker, and at 24 h, it shifted to the vasculature. This suggests that *YUC8* not only respond to temperature in terms of their induction or repression but can also be regulated spatiotemporally.

The differences in expression patterns among the *YUC* genes suggest functional divergence within this gene family. The early and transient response of *YUC9* contrasts with the more sustained response of *TAA1*, indicating that these genes might play distinct roles in mediating temperature-dependent root development.

These specific modifications in the expression of IPyA pathway genes in the root meristem suggest that local auxin biosynthesis might play a major role in the root system response to increasing temperatures.

Nevertheless, we noted a slight discrepancy between auxin accumulation levels, or in other words, *DR5:GUS* staining intensities and the upregulation of auxin biosynthesis genes expression levels at 34 ºC. *DR5:GUS* reporter line showed a repression of expression levels at 34 ºC. This divergence suggests that the relationship between auxin biosynthesis and auxin response is more complex than just a simple correlation between gene expression levels. While the induction of biosynthesis genes such as *TAA1*, *YUC3*, *YUC7*, *YUC8*, and *YUC9* at 34 ºC suggested the potential increase of auxin production, other regulatory mechanisms may counteract this effect, leading to a reduced auxin accumulation as reported by *DR5* activity.

One plausible explanation could involve an active catabolism or conjugation of auxin. Auxin catabolic pathways, including the actions of enzymes like *DAO1*. We have demonstrated that *DAO1* expression is upregulated in response to increasing temperatures, perhaps to prevent excessive auxin accumulation. This possibility aligns with the idea that plants need to fine-tune auxin levels to balance growth and stress responses, especially under stressful environmental conditions

5.4. *DAO1* expression in *Arabidopsis* roots in response to temperature

The expression of *DAO1p:GUS* reporter lines showed increasing levels up to the 34 ºC (Figure 13). This observed increase on *DAO1* expression levels could explain why *DR5* levels are lower, or why there is a reduction on auxin accumulation, at 34 ºC despite the induction of the IPyA biosynthesis pathway genes. However, *DAO1* expression level differences are not statistically significant, and we cannot conclude that the *DAO1* expression induction at 34 ºC is sufficient to explain the decrease in auxin accumulation.

Auxin catabolism is also regulated by specific genes, such as those belonging to the *GRETCHEN HAGEN 3* (*GH3*) family. These genes play a key role in the conjugation of IAA with amino acids, leading to auxin inactivation. The induction of *GH3* expression is triggered by various factors, including temperature stress in seedlings. According to the review by Luo et al. (2023), *GH3* genes exhibit a notable response to high temperatures in *Arabidopsis*. This suggests that auxin conjugation may play an important role in explaining the

differences in expression levels observed between *DR5* and auxin biosynthesis genes under high-temperature conditions.

The expression pattern of *DAO1* in the root is very homogeneous, making it challenging to observe differences in staining levels by simple visual inspection (Figure 13A). as previously described by Zhang et al. (2017), *DAO1* plays a constitutive role in maintaining auxin homeostasis under non-stressful conditions. This constitutive expression, observed in most tissues during normal growth and particularly prominent in reproductive organs during flower opening, could explain the high expression levels observed for *DAO1* in our temperature assays. We have reduced the staining time and normalized the GUS staining levels using ImageJ, but we were unable to detect significant differences between the various temperatures used.

5.5. *In silico* analysis: identification of potential TFs of interest

Our combined analysis of ChIP-seq and DAP-seq datasets highlights potential transcription factors (TFs) involved in the regulation of genes in the IPyA pathway. By identifying common TFs in both datasets, we can prioritize candidates for further experimental validation to understand their regulatory roles in modulating the levels of expression of IPyA pathway genes under different temperature conditions.

For *TAA1*, TFs from the bZIP (ABFs), bHLH, and MYB families were consistently identified in both ChIP-seq and DAP-seq analyses. These TFs are known to regulate responses to abiotic stresses, such as temperature and water deficit, making them strong candidates for further study. Similarly, *TAR2* also showed consistent association with TFs from the MYB family in both datasets. The MYB family's involvement in stress responses, including salinity and drought, aligns with the potential roles of *TAR2* in adapting to environmental changes.

For *YUC3*, TFs from the HD-ZIP family, specifically HB members (such as ATBH13), were found in both datasets. These TFs are associated with developmental processes and stress responses, suggesting a multifaceted role in regulating *YUC3*. In *YUC6*, MYB and bZIP TFs were consistently identified across the datasets, further supporting their importance in controlling auxin biosynthesis.

Interestingly, no common TFs were identified between ChIP-seq and DAP-seq for *YUC7, YUC8,* or *YUC9.* This lack of overlap may suggest that the TFs binding these genes are context-dependent, with ChIP-seq capturing interactions *in vivo* under specific conditions and DAP-seq providing broader *in vitro* interactions, or maybe not every TF identified employing ChIP-seq was also investigated in the DAP-seq assays.

For that reason, DREB2A could also be a good candidate for our study. Although, it does not appear in DAP-seq data. DREB2A, a bHLH TF identified in the ChIP-seq dataset for *TAA1* and *YUC6,* had a relevant role in heat acclimation and the regulation of genes involved in abiotic stress responses (Sakuma et al., 2006). Given the critical role of temperature in modulating plant growth and development, it is possible that DREB2A contributes to the regulation of the IPyA pathway genes in *Arabidopsis*.

Further investigation is required to evaluate whether DREB2A directly modulates the expression of *TAA1*, *YUC6*, or other IPyA pathway genes under heat stress conditions. This could involve phenotypic analysis of *dreb2a* mutant lines or lines with inducible expression of this TF under temperature stress, combined with transcriptomic studies to assess its impact on the expression levels of the IPyA pathway genes. Such experiments would provide valuable insights into the potential regulatory role of DREB2A and its influence on auxin biosynthesis in response to temperature fluctuations.

For any additional candidate TFs identified, similar strategies can be followed to study their function. Their regulatory roles can be evaluated by analyzing phenotypes of mutant and inducible lines. Quantifying their effects on the expression levels of genes in the IPyA biosynthesis pathway will provide deeper insights into their regulatory impact.

In conclusion, the TFs identified as common in both datasets, particularly those associated with *TAA1*, *TAR2*, *YUC3*, and *YUC6*, represent promising targets for future research. Their consistent presence across ChIP-seq and DAP-seq underscores their potential relevance in regulating auxin biosynthesis and related stress responses.

6. Conclusions

This study provides new insights into how temperature changes modify auxin levels and, consequently, root architecture in *A. thaliana*.

We quantified major root phenotypic parameters in response to increasing temperatures in control and mutants with impaired auxin production. We then characterized the expression levels of *DR5* reporter gene and IPyA pathway genes under different temperatures (20 ºC, 28 ºC, 34 ºC, and 40 ºC). Due to the only partial correlation between the expression levels of *DR5* and the auxin biosynthesis genes under specific temperature conditions, we investigated molecular mechanisms that might interfere with auxin accumulation, such as temperature-dependent regulation of the IAA catabolism gene *DAO1*. Complementing our work, we performed an *in silico* analysis of candidate TFs that could modulate auxin levels.

Based on our work, we can conclude the following:

6.1. Temperature shape root architecture in WT *Arabidopsis* seedlings. At 28 ºC, primary root elongation is promoted and the lateral root number increased. However, at 34 ºC (or higher), root growth is inhibited, and the number of lateral root decrease significantly. Auxin biosynthesis mutants exhibit altered phenotypes: the single mutant *wei8-1* did not display a significant difference compared to WT, but the double mutant *wei8-1 tar2-1* showed a compromised root development. These findings highlight the essential role of auxin production in root adaptation to elevated temperatures.

6.2. *DR5* reporter activity showed temperature-dependent dynamics, with enhanced auxin responses at 28 °C and a repression of expression levels at 34 °C, more evident at prolonged exposure times or higher temperatures. These patterns suggest distinct regulatory mechanisms for auxin homeostasis under thermomorphogenesis and heat stress.

6.3. Genes involved in the IPyA pathway (*TAA1/TAR2* and *YUCs*) showed different expression patterns and levels depending on temperature. In general, these genes were locally induced at 34 ºC, but auxin response decrease at that temperature, suggesting that other molecular mechanisms play a role in regulating auxin avaiability.

6.4. The auxin catabolism gene *DAO1* showed a slightly induction of expression levels at high temperatures, suggesting that *DAO1* could be responsible, at least in part, of the decrease in auxin levels observed at 34 ºC.

6.5. *In silico* analyses identified several candidate TFs potentially regulating IPyA biosynthesis pathway. Shared TFs between *TAA1/TAR2* and *YUCs* suggest their potencial role in coordinating auxin synthesis under different temperatures, contributing to root adaptability.

These results underscore the critical importance of auxin biosynthesis and the IPyA biosynthesis pathway genes expression regulation in maintaining root architecture under environmental cues.

7. Bibliographic references

Agusti, J., Ramireddy, E., & Brumos, J. (2021). Editorial: Integration of Hormonal Signals Shaping Root Growth, Development, and Architecture. In *Frontiers in Plant Science* (Vol. 12). Frontiers Media S.A. https://doi.org/10.3389/fpls.2021.634066

Ai, H., Bellstaedt, J., Bartusch, K. S., Eschen-Lippold, L., Babben, S., Balcke, G. U., Tissier, A., Hause, B., Andersen, T. G., Delker, C., & Quint, M. (2023). Auxin-dependent regulation of cell division rates governs root thermomorphogenesis. *The EMBO Journal*, *42*(11). https://doi.org/10.15252/embj.2022111926

Blakeslee, J. J., Spatola Rossi, T., & Kriechbaumer, V. (2019). Auxin biosynthesis: Spatial regulation and adaptation to stress. In *Journal of Experimental Botany* (Vol. 70, Issue 19, pp. 5041–5049). Oxford University Press. https://doi.org/10.1093/jxb/erz283

Brumos, J., Alonso, J. M., & Stepanova, A. N. (2014). Genetic aspects of auxin biosynthesis and its regulation. In *Physiologia Plantarum* (Vol. 151, Issue 1, pp. 3–12). Blackwell Publishing Ltd. https://doi.org/10.1111/ppl.12098

Brumos, J., Robles, L. M., Yun, J., Vu, T. C., Jackson, S., Alonso, J. M., & Stepanova, A. N. (2018). Local Auxin Biosynthesis Is a Key Regulator of Plant Development. *Developmental Cell*, *47*(3), 306-318.e5. https://doi.org/10.1016/j.devcel.2018.09.022

Brumos, J., Zhao, C., Gong, Y., Soriano, D., Patel, A. P., Perez-Amador, M. A., Stepanova, A. N., & Alonso, J. M. (2020). An Improved Recombineering Toolset for Plants. *Plant Cell*, *32*(1), 100–122. https://doi.org/10.1105/tpc.19.00431

Calleja-Cabrera, J., Boter, M., Oñate-Sánchez, L., & Pernas, M. (2020). Root Growth Adaptation to Climate Change in Crops. In *Frontiers in Plant Science* (Vol. 11). Frontiers Media S.A. https://doi.org/10.3389/fpls.2020.00544

Cao, X., Yang, H., Shang, C., Ma, S., Liu, L., & Cheng, J. (2019). The roles of auxin biosynthesis YUCCA gene family in plants. In *International Journal of Molecular Sciences* (Vol. 20, Issue 24). MDPI AG. https://doi.org/10.3390/ijms20246343

Chen, Q., Dai, X., De-Paoli, H., Cheng, Y., Takebayashi, Y., Kasahara, H., Kamiya, Y., & Zhao, Y. (2014). Auxin overproduction in shoots cannot rescue auxin deficiencies in arabidopsis roots. *Plant and Cell Physiology*, *55*(6), 1072–1079. https://doi.org/10.1093/pcp/pcu039

Geisler, M. M. (2021). A Retro-Perspective on Auxin Transport. *Frontiers in Plant Science*, *12*. https://doi.org/10.3389/fpls.2021.756968

González-García, M. P., Conesa, C. M., Lozano-Enguita, A., Baca-González, V., Simancas, B., Navarro-Neila, S., Sánchez-Bermúdez, M., Salas-González, I., Caro, E., Castrillo, G., & del Pozo, J. C. (2023).

Temperature changes in the root ecosystem affect plant functionality. *Plant Communications*, *4*(3). https://doi.org/10.1016/j.xplc.2022.100514

Karlova, R., Boer, D., Hayes, S., & Testerink, C. (2021). Root plasticity under abiotic stress. *Plant Physiology*, *187*(3), 1057–1070. https://doi.org/10.1093/plphys/kiab392

Kleine-Vehn, J., & Sauer, M. (n.d.). *Plant Hormones Methods and Protocols Third Edition Methods in Molecular Biology 1497*. http://www.springer.com/series/7651

Luo, P., & Di, D. W. (2023). Precise Regulation of the TAA1/TAR-YUCCA Auxin Biosynthesis Pathway in Plants. In *International Journal of Molecular Sciences* (Vol. 24, Issue 10). Multidisciplinary Digital Publishing Institute (MDPI). https://doi.org/10.3390/ijms24108514

Luo, P., Li, T. T., Shi, W. M., Ma, Q., & Di, D. W. (2023). The Roles of GRETCHEN HAGEN3 (GH3)-Dependent Auxin Conjugation in the Regulation of Plant Development and Stress Adaptation. In *Plants* (Vol. 12, Issue 24). Multidisciplinary Digital Publishing Institute (MDPI). https://doi.org/10.3390/plants12244111

Mashiguchi, K., Tanaka, K., Sakai, T., Sugawara, S., Kawaide, H., Natsume, M., Hanada, A., Yaeno, T., Shirasu, K., Yao, H., McSteen, P., Zhao, Y., Hayashi, K. I., Kamiya, Y., & Kasahara, H. (2011). The main auxin biosynthesis pathway in Arabidopsis. *Proceedings of the National Academy of Sciences of the United States of America*, *108*(45), 18512–18517. https://doi.org/10.1073/pnas.1108434108

Muraro, D., Byrne, H., King, J., & Bennett, M. (2013). The role of auxin and cytokinin signalling in specifying the root architecture of Arabidopsis thaliana. *Journal of Theoretical Biology*, *317*, 71–86. https://doi.org/10.1016/j.jtbi.2012.08.032

Rueden, C. T., Schindelin, J., Hiner, M. C., DeZonia, B. E., Walter, A. E., Arena, E. T., & Eliceiri, K. W. (2017). ImageJ2: ImageJ for the next generation of scientific image data. BMC Bioinformatics, 18(1), 529. https://doi.org/10.1186/s12859-017-1934-z

Overvoorde, P., Fukaki, H., & Beeckman, T. (2010). Auxin control of root development. In *Cold Spring Harbor perspectives in biology* (Vol. 2, Issue 6). https://doi.org/10.1101/cshperspect.a001537

Sakuma, Y., Maruyama, K., Qin, F., Osakabe, Y., Shinozaki, K., & Yamaguchi-Shinozaki, K. (2006). *Dual function of an Arabidopsis transcription factor DREB2A in water-stress-responsive and heat-stress-responsive gene expression*. www.pnas.orgcgidoi10.1073pnas.0605639103

Stepanova, A. N., Robertson-Hoyt, J., Yun, J., Benavente, L. M., Xie, D. Y., Doležal, K., Schlereth, A., Jürgens, G., & Alonso, J. M. (2008). TAA1-Mediated Auxin Biosynthesis Is Essential for Hormone Crosstalk and Plant Development. *Cell*, *133*(1), 177–191. https://doi.org/10.1016/j.cell.2008.01.047

Stepanova, A. N., Yun, J., Robles, L. M., Novak, O., He, W., Guo, H., Ljung, K., & Alonso, J. M. (2011). The Arabidopsis YUCCA1 Flavin Monooxygenase functions in the Indole-3-Pyruvic acid branch of Auxin Biosynthesis. *Plant Cell*, *23*(11), 3961–3973. https://doi.org/10.1105/tpc.111.088047

Tanaka, H., Dhonukshe, P., Brewer, P. B., & Friml, J. (2006). Spatiotemporal asymmetric auxin distribution: A means to coordinate plant development. In *Cellular and Molecular Life Sciences* (Vol. 63, Issue 23, pp. 2738–2754). https://doi.org/10.1007/s00018-006-6116-5

Wong, C., Alabadí, D., & Blázquez, M. A. (2023). Spatial regulation of plant hormone action. In *Journal of Experimental Botany* (Vol. 74, Issue 19, pp. 6089–6103). Oxford University Press. https://doi.org/10.1093/jxb/erad244

Zhang, J., Lin, J. E., Harris, C., Pereira, F. C. M., Wu, F., Blakeslee, J. J., & Peer, W. A. (2016). DAO1 catalyzes temporal and tissue-specific oxidative inactivation of auxin in Arabidopsis thaliana. *Proceedings of the National Academy of Sciences of the United States of America*, *113*(39), 11010–11015. https://doi.org/10.1073/pnas.1604769113

Zhang, Y., Yu, J., Xu, X., Wang, R., Liu, Y., Huang, S., Wei, H., & Wei, Z. (2022). Molecular Mechanisms of Diverse Auxin Responses during Plant Growth and Development. In *International Journal of Molecular Sciences* (Vol. 23, Issue 20). MDPI. https://doi.org/10.3390/ijms232012495

Supplemental figures

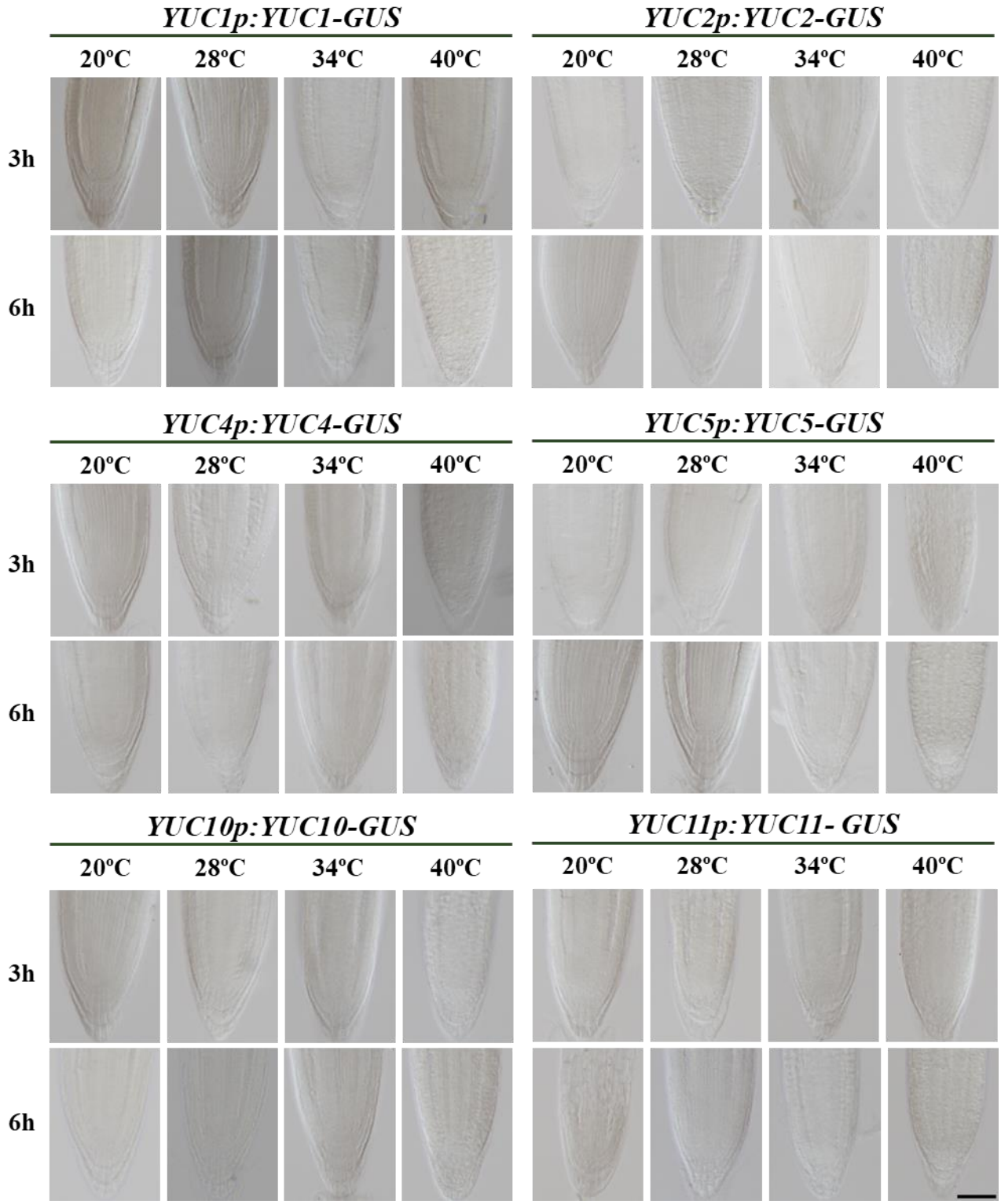

Supplemental Fig. 1. Absence of *YUCs* gene expression under varying temperature conditions. Representative pictures of root apical meristem of *Arabidopsis* 7-day-old seedlings under temperature treatment for 3 and 6 h. Histochemical GUS staining revealed no detectable GUS activity at any of the tested temperatures. Scale bar = 50 µm